INSTITUTE FOR FUSION STUDIES

DOE/ET-53088-519 IFSR #519

PROCEEDINGS

US-JAPAN WORKSHOP ON
NUCLEAR FUSION IN DENSE PLASMAS

edited by

S. ICHIMARU
Department of Physics
University of Tokyo

T. TAJIMA
Institute for Fusion Studies
The University of Texas at Austin

October 1991

THE UNIVERSITY OF TEXAS

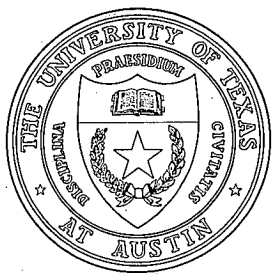

AUSTIN

PROCEEDINGS

1991 US-JAPAN WORKSHOP

ON

NUCLEAR FUSION IN DENSE PLASMAS

edited by

S. ICHIMARU
Department of Physics
University of Tokyo

T. TAJIMA
Institute for Fusion Studies
The University of Texas at Austin

Workshop Sponsored by
Joint Institute for Fusion Theory

October 7-9
Joe C. Thompson Conference Center
The University of Texas at Austin

TABLE OF CONTENTS

I. About The Workshop

The planning of the US-Japan Joint Institute for Fusion Theory (JIFT) Workshop on Nuclear Fusion in Dense Plasmas was initiated in March, 1990, when one of the organizers, Professor S. Ichimaru, in consultation with Professor D. Baldwin, then Director of the Institute for Fusion Studies, Austin, Texas, Professor W. Horton, and the other organizer, T. Tajima, prepared a proposal, and submitted it to Professor Y.H. Ichikawa of the National Institute for Fusion Science, Nagoya, Japan. The objectives of the Workshop stated in the proposal were as follows: "In condensed-matter systems such as shock compressed plasmas, ultrahigh pressure metals, metal hydrides and interiors of dense stars, collections of ionized nuclei and electrons constitute dense plasmas, which exhibit various changes in the microscopic structures; these in turn control vital elements of the system properties such as the nuclear reaction rates, opacities, transport processes and mechanical properties. At the Workshop, participants from both sides will discuss the latest progress achieved in their respective fields of condensed plasmas, and thereby elucidate the physical mechanisms of those elementary processes in such strongly correlated systems. The fields to be covered are centered in plasma and fusion physics, but are also closely connected with nuclear physics, atomic and molecular physics, condensed matter and astrophysics; the subject is interdisciplinary in its character."

The Workshop was approved by the JIFT Steering Committee in November, 1990, and was held in Austin, Texas, October 7-9, 1991. It was the latest in a series of ~36 JIFT Workshops (I-29) held since the inception of JIFT in 1979; and was timely in that it addressed fresh theoretical and experimental results in the field of nuclear fusion in dense plasmas and associated areas.

The scientific areas covered at the Workshop may be classified into the following subfields: (i) basic theory of dense plasma physics and its interface with atomic physics and nuclear physics; (ii) physics of dense z-pinches, ICF plasmas etc; (iii) stellar interior plasmas; (iv) cold fusion; (v) other dense plasmas.

Judging from the amount and quality of discussion during the Workshop and from the remarks made by the participants at the concluding discussion and summary, we may conclude the main purpose of the Workshop was accomplished, to the extent that we brought together active researchers from a wide range of subfields in nuclear fusion in dense plasmas and from associated fields to communicate with each other in a friendly, scientific, and yet critical manner so as to widen and deepen our understanding of these respective fields. We covered many

relevant fields, including the basic statistical physics of dense plasmas, atomic physics of dense plasmas, metals and associated condensed matter physics, thermonuclear fusion and associated processes in dense z-pinches, electrostatic confinement, inertial confinement and other configurations, some aspects of nuclear physics of fusion, numerical simulations of dense plasmas, nuclear fusion in stellar and planetary interiors, nucleosynthesis in the Universe, neutrino physics in dense plasmas, cluster impact fusion, laser ablated plasmas, and cold fusion. These topics vary widely, but share some common physics. This Workshop, we believe, facilitated the coming together of experts from various subfields and succeeded in inspiring new thinking in the participants.

In the following we present a snapshot of the Workshop consisting of the opening remarks of the Director of the Institute for Fusion Studies, the Workshop program, abstracts of the talks, and a list of addresses of the speakers and participants.

Before closing, the Organizers would like to thank Professor Y.H. Ichikawa and Professor W. Horton for their consultation and assistance, and Joan Gillette for her untiring dedication in running the Workshop smoothly. The Workshop was sponsored by JIFT and was in part supported by a grant from the U.S. Department of Energy, DE-FG05-80ET53088.

II. OPENING REMARKS–PROFESSOR HAZELTINE

On behalf of the Institute for Fusion Studies, Welcome to Austin. Professors Ichimaru and Tajima are to be congratulated for what is clearly to be a very exciting conference. I envy you.

I heard my first technical talk about fusion when I was a graduate student, 25 years ago, at the University of Michigan. My thesis work in field theory had nothing to do with plasma or fusion, but I was beginning to get interested in the fusion program.

I don't remember who gave the talk—when you don't know anyone, you forget names. But I actually remember the talk quite well; it made an impression. For even in my ignorance I realized that it was outside the standard orthodoxy. It proposed an unconventional approach to fusion, involving the electrostatic confinement of hydrogen ions. I didn't understand the details, but I remember the speaker's emphasis that confining *ions* was all that mattered for fusion.

I was impressed by the talk because I believed, like many graduate students, that a characteristic of the best physics was venturing off the beaten path. And also like many graduate students I found it easy and fun to suspect that the army of scientists pursuing conventional fusion was misguided. The impressive thing was imagination: seeing a better way, especially an unexpected better way.

Of course orthodoxies are often close to the mark, and even graduate students can occasionally err. So I am not too embarrassed to admit that most of my own work in fusion has followed the program mainstream. But the brash confidence of a beginning scientist seems to me more precious and constructive than ever. Intellectual contraction of the fusion program during the past five or ten years, allowing for fewer and more similar devices, and focussing theory on a narrower set of issues, give it special importance.

It is routine, and fitting, to complain that the front of fusion research has become too narrow. The need for breadth in the program was a primary motivation for founding the Institute for Fusion Studies, and it was clearly one of the motivations for this Workshop. However the boldness and open-mindedness that impressed me in that talk involves more than breadth. It also reflects faith–faith that there are still brilliant vistas and miraculous shortcuts to be found, off the beaten track.

Of course that first talk I heard about fusion would have fit very well into this Workshop; indeed, it was reading the abstract of Professor Miley's contribution that reminded me of it. For your program is indeed broad, including stellar plasmas, z-pinch physics and even cold fusion. And it contains many examples of imagination, boldness and faith.

As I said a moment ago, I envy you. Thank you very much for coming.

III. PROGRAM

1991 US-JAPAN WORKSHOP ON NUCLEAR FUSION IN DENSE PLASMAS

(Sponsored by Joint Institute for Fusion Theory)

October 7-9
Joe C. Thompson Conference Center
The University of Texas at Austin

SUNDAY EVENING *8:00-10:00 O'Clock, Cocktails, (Cash Bar)*
Guest Quarters Suite Hotel, Lounge Area, First Floor

MONDAY MORNING–(CHAIRMAN, T. TAJIMA)
(All Sessions, Room 1.110, Thompson Conference Center)

R. Hazeltine	9:00	*Opening Remarks*
S. Ichimaru	9:30	*Review Talk: Nuclear Fusion in Dense Plasmas–Supernovae to Ultrahigh Pressure Liquid Metals*
	10:30	*Break*
G. Miley	11:00	*Dense Core Plasma in an Inertial Electrostatic Confinement Device*
C. Wheeler	11:30	*Thermonuclear Carbon Ignition in Electron Degenerate Stars*
	12:00	*Lunch*

MONDAY AFTERNOON–(CHAIRMAN, N. ROSTOKER)

H. Van Horn	1:30	*Helium 'Burning' at T = 0 and Ultra-High Densities*
S. Ogata	2:00	*Nuclear Reaction Rates in Dense Multi-Ionic Stellar Materials*
J. Vary	2:30	*Model for Cluster Impact Fusion*
	3:00	*Break*
M. Takita	3:30	*Preliminary Results of Cold Fusion Experiment from Kamiokande*
S. Jones	4:00	*Anomalous Nuclear Effects in Deuterided Solids–Preliminary New Results*

MONDAY EVENING *7:00-9:00 O'Clock, Banquet*
Guest Quarters Suite Hotel, "Houston I" Room

TUESDAY MORNING–(CHAIRMAN, H. VAN HORN)

N. Rostoker	9:00	*Radiative Collapse of a Dense Plasma*
K. Nishihara	9:30	*Effect of Radiative Processes on Radiation Transport in Laser Produced High-Z Plasma*
I. Lindemuth	10:00	*Magnetized Target Fusion*
	10:30	*Break*
R. More	11:00	*Semiclassical Calculation of Dense Plasma Physics*
S. Ichimaru	11:30	*Liquid Metallic Hydrogen–Equation of State, Transport, and Impurity Ionization*
	12:00	*Lunch*

TUESDAY AFTERNOON–(CHAIRMAN, K. NISHIHARA)

F. Rogers	1:30	*Opacity in Stellar Plasmas*
H. Iyetomi	2:00	*Freezing Transitions and Phase Separations in Dense Multi-Ionic Plasmas*
J. Benage	2:30	*Electrical Resistivity of a Dense Polyurethane Plasma*
	3:00	*Break*
J. Shlachter	3:30	*Dense Plasmas Produced from Solid Deuterium Z-Pinches*
M. McKubre	4:00	*Electrochemistry and Calorimetry of the D/Pd System*
E. Cecil	4:30	*Gamma-Rays and Charged Particle Studies from Dense Plasmas*

WEDNESDAY MORNING–(CHAIRMAN, N. ITOH)

J. Weisheit	9:00	*On the Rate of Ionization in Dense Plasmas*
K. Nishihara	9:30	*Nonlinear AC Conductivity of Solid Density Plasma*
S. Younger	10:00	*Many-Atom Effects and Transport Processes in Dense Plasmas*
	10:30	*Break*
M. Takita	11:00	*Recent Results of ^{8}B Solar Neutrino Observation from Kamiokande*
M. Downer	11:30	*Dense Plasmas Created by Femtosecond Laser Pulses*
	12:00	*Lunch*

WEDNESDAY AFTERNOON–(CHAIRMAN, J. WEISHEIT)

N. Itoh	1:30	*Neutrino Energy Loss in Dense High-Temperature Stars*
R. Matzner	2:00	*Baryon Inhomogeneities and the Primordial Light-Element Abundances*
P. Hagelstein	2:30	*Coherent and Semi-Coherent Neutron Transfer Reactions*
S. Mahajan		*Modes in Gluon and Quark-Gluon Plasmas*
		(CHAIRMEN, T. TAJIMA AND S. ICHIMARU)
	3:30	*Discussion and Summary*
	4:30	*Lab Tours*

IV. ABSTRACTS OF THE PRESENTATIONS

ELECTRICAL RESISTIVITY OF A DENSE POLYURETHANE PLASMA*

John F. Benage, Jr.

Physics Division
Los Alamos National Laboratory
Los Alamos, NM 87545

Abstract

We have measured the electrical resistivity of a dense polyurethane plasma that is produced in a capillary discharge. These discharges are produced by passing a large current, 250 kA, through a 20 micron hole in a block of polyurethane. The current causes material to be ablated off the wall that is then ohmically heated, producing a plasma with density of 5×10^{21} cm^{-3} and a temperature of 25-30 eV. The resistivity is determined by measuring the voltage across the plasma, the current through it, and the size of the discharge channel. To compare our results to the many theories of dense plasmas, we must also determine the density and temperature. The temperature is measured using an x-ray pinhole framing camera and the density is determined from calculations using a sophisticated 1-D MHD model. We compare our results to several theories and find that the resistivity we measure is higher than predicted for each case. We also find that the MHD model cannot predict the size of the discharge channel as accurately as we expect. This leads us to conclude that the pressure in the discharge is not given by the ideal gas law but is slightly less, as some have predicted. Ongoing experiments on dense aluminum and copper plasmas will also be discussed.

*Work performed under the auspices of the U. S. Department of Energy.

ABSTRACT SUBMITTED

U.S.-Japan Cooperative Workshop on Nuclear Fusion in Dense Plasmas
October 7-9, 1991. University of Texas at Austin

Gamma rays and charged particle studies from dense plasmas* F.E. Cecil, H. Liu, J.C. Scorby, J.A. McNeil and C.S. Galovich[a]. Colorado School of Mines.
Recent measurements of cross sections for the radiative capture reactions of protons and deuterons on ^{2}H, ^{3}H, ^{3}He, ^{6}Li, ^{7}Li, ^{9}Be, and ^{11}B at bombarding energies between 20 and 180 keV will be summarized. Comparisons of some of these reactions to distorted-wave Born approximation calculations will be made. Applications of the reactions to the diagnostics of hot and cold fusion experiments will be discussed. Measurements of the charged particle reactions D(d,p)T, D(d,n)^{3}He, $^{6}Li(d,p)^{7}Li$, and $^{6}Li(d,\alpha)^{4}He$ down to center-of-mass energies of 2 keV will likewise be described. Possible evidence for Oppenheimer-Phillips or electron-screening type enhancement of some of these reactions will evaluated. Implications of these reactions to the production of measureable amounts of heat in the absence of significant escaping radiation will be considered. We will also describe our efforts at observing energetic charged particles from gas loaded Ti-D foils and from deuterium glow discharge devices.
* Supported by the U.S. Department of Energy and the Electric Power Research Institute.

[a]Permanent address: University of Northern Colorado.

*RADIATIVE COLLAPSE OF A KRYPTON Z-PINCH PLASMA**

J. DAVIS
RADIATION HYDRODYNAMICS BRANCH
PLASMA PHYSICS DIVISION
NAVAL RESEARCH LABORATORY
WASHINGTON, DC 20375

The concept of pulsed-power driven Z-pinch radiative collapse has attracted considerable attention recently because of its potential as a broadband radiation source as well as for investigating fundamental physical processes in dense and strongly coupled plasmas. In this investigation the dynamic evolution of a krypton gas puff plasma is explored as it implodes self-consistently under the influence of megamperes of current produced by a SATURN class generator. The numerical simulations are performed using a non-LTE radiation hydrodynamics model including the dense plasma effects on atomic rate coefficients and degeneracy.

* *Work supported by ONR.*

WAS NOT ABLE TO ATTEND MEETING

DENSE PLASMAS CREATED BY FEMTOSECOND LASER PULSES

M.C. DOWNER

Department of Physics
The University of Texas at Austin
Austin, Texas 78712

ABSTRACT

Femtosecond laser pulses can create plasmas up to solid density with optically sharp interfaces by heating a solid target faster than hydrodynamic surface expansion occurs. We report experiments which measure the quasi-equilibrium properties and dynamical evolution of carbon, tungsten, aluminum and silver plasmas by time-resolved optical reflectance and thermionic electron emission methods.

* * * * * * * * * * *

COHERENT AND SEMI-COHERENT NEUTRON TRANSFER REACTIONS

Peter L. Hagelstein

Massachusetts Institute of Technology
Research Laboratory of Electronics
Cambridge, Massachusetts 02139

Abstract

We have examined mechanisms for the coherent neutron capture onto, and the coherent neutron removal from nuclei in the presence of a lattice. Under a fairly restrictive circumstances, it is possible to satisfy both energy and momentum conservation requirements between the microscopic nuclear system and the macroscopic lattice such that coherent nuclear energy transfer (associated with a neutron transition) to and from the lattice may occur.

This mechanism enables coherent neutron donor and acceptor reactions to occur, with deuterium as the optimum donor nucleus. Coherent reaction pathways leading to heat, tritium, and helium generation are proposed: Heat generation in Pons-Fleischmann cells would result from coherent neutron capture onto ^{6}Li in the lattice; tritium generation would result from coherent neutron capture onto deuterium; coherent neutron capture onto ^{7}Li would lead to ^{8}Li, which would beta decay to ^{8}Be, and ultimately alpha decay to form two ^{4}He nuclei.

Semi-coherent reactions, in which the neutron capture part of the reaction would yield energetic products, are also proposed to account for fast triton production and secondary fast neutron generation.

NUCLEAR FUSION IN DENSE PLASMAS: SUPERNOVAE TO ULTRAHIGH-PRESSURE LIQUID METALS

Setsuo Ichimaru
Department of Physics, University of Tokyo
Bunkyo, Tokyo 113, Japan

This review begins with classifying the reactions in three elements: *binary processes*, *few-particle processes*, and *many-particle processes*, to elucidate the special features for the *nuclear fusion in dense plasmas*. These analyses are then applied to the estimation for nuclear reaction rates in the specific examples of dense plasmas,[1] namely, ^{12}C-^{12}C reactions in a white-dwarf progenitor of supernova (SN), p-p reactions in the solar interior (SI), d-d reactions in palladium hydride (MH), and p-d or p-^{7}Li reactions in pressurized liquid metals (PM). It is stressed that the nuclear reactions in supernovae and in the ultrahigh-pressure liquid metals are similar in that both depend strongly on the many-particle processes. Table I lists definition and the assumed or calculated values for some of the quantities in those dense plasmas.

In analyzing the nuclear reactions in dense plasmas, we single out reacting (R) nuclei, i and j, and name all others as "spectator (S)" nuclei. In addition to those "R" and "S" nuclei, the system contains electrons (and muons). The S-wave scattering between "R" nuclei with relative kinetic energy E is described by the Schrödinger equation

$$\left[-\frac{\hbar^2}{2\mu_{ij}}\frac{d^2}{dr^2} + W_{ij}(r) - E \right] r\,\psi_{ij}(r) = 0 , \qquad (1)$$

where $W_{ij}(r)$ is the effective potential of scattering and μ_{ij} denotes the reduced mass. Nuclear reaction rate at E is given by[2,3]

$$R_{ij}(E) = \frac{8 S_{ij} r_{ij}^*}{(1+\delta_{ij})\hbar}\frac{n_i n_j}{n_i + n_j}|\psi_{ij}(0)|^2 , \qquad (2)$$

where $r_{ij}^* = \hbar^2/2\mu_{ij}Z_iZ_je^2$ are the nuclear "Bohr radii". The reaction rates at temperature T are finally obtained through an "R" average:

$$R_{ij}(T) = R_{ij}(E)_R \qquad (3)$$

over the states of "R" nuclei.

BINARY PROCESSES When $W_{ij}(r) = W_0(r) = Z_i Z_j e^2/r$ in (1), Eq. (3) gives the Gamow reaction rate,

$$R_G = \frac{32 S_{ij} r_{ij}^* n_j \tau_{ij}}{3^{3/2}(1 + \delta_{ij})\hbar} \exp(-\tau_{ij}), \quad (4)$$

where $\tau_{ij} = 3(\pi/2)^{2/3}(E_G/T)^{1/3}$ and $E_G = Z_i Z_j e^2/r_{ij}^*$. $E_G >> T$ has been assumed in the derivation of (4).

FEW-PARTICLE PROCESSES The presence of electrons or other leptons acts to modify (*i.e.*, screen) the Coulombic repulsion from $W_0(r)$ to $W_S(r)$. In the short range, one expands $W_S(r)$ and defines a screening distance D_S via $W_S(r) = W_0(r)[1 - r/D_S \cdots]$. A 1s-electron with an effective mass m^*, for instance, may bring about $D_S \approx \hbar^2/m^* Z_j e^2$. If $Z_i Z_j e^2/D_S >> T$ (*i.e.*, "cold fusion"), as in the present MH and PM cases, Eq. (4) is replaced by[4]

$$R_S = \frac{8 S_{ij} r_{ij}^* n_j}{(1 + \delta_{ij})\hbar} \exp\left(-\pi \sqrt{\frac{D_S}{r_{ij}^*}}\right). \quad (5)$$

If not, the electron screening can give rise to only a small perturbation[5] to Eq. (4). Note that Eq. (5) is independent of T, in line with the original idea[6] for the *pycnonuclear reactions.* The analysis is applicable irrespective of whether the "R" nuclei are in a fluid, molecular, or crystalline state. These are the extent to which the leptons may affect the nuclear reactions.

MANY-PARTICLE PROCESSES The most significant effects in dense plasmas are those of the screening potentials[7]

$$H_{ij}(r) = W_S(r) + T \ln[g_{ij}(r)], \quad (6)$$

produced collectively through averages over the "S" nuclei, where $g_{ij}(r)$ denote the resultant joint probability densities for the "R" pairs. When "R" and "S" nuclei are in classical fluid states with $\Lambda_{ij} < 1$, one can determine $H_{ij}(r)$ accurately through analyses[3,5] combining between Monte Carlo (MC) sampling and solutions to the fluid integral equations. The *enhancement factors* for the reaction rates over Eq. (4) or (5) are then given by

$$A_{ij} = \exp\{\langle H_{ij}(r)/T \rangle\}, \quad (7)$$

where $\langle \cdots \rangle$ means a path-integral "R" average with respect to the penetrating wave functions from $r = 0$ to the classical turning radii and back.[10] This average can be evaluated through an exact solution[3] to Eq. (1). It should be remarked that $H_{ij}(0)$ correspond to the increments in the Coulombic chemical potentials for the "R" pair before and after the reactions.[8,9] Approximately, one finds[1,2,3,9]

$$H_{ij}(0) \approx 1.06 \times \Gamma_{ij}^S. \quad (8)$$

In the cases of SN, the basic reaction rates are R_G. SN mechanisms[2,3,5] depend strongly on enhancement due to the many-particle processes.

In SI, the basic reaction rates are R_G. No significant enhancement is expected either from electron screening or from the many-particle processes. Such is the case[11] also with the inertial-confinement fusion plasmas.

In MH, the reacting nuclei (deuterons, in the present example) are under a strong influence of the inhomogenious lattice field produced by the metal (palladium) atoms; due care[4] must therefore be exercised in the MC sampling of the screening potentials via Eq. (6). MH may employ the enhancement (7) and thereby raise the reaction rate to a barely observable level ($\simeq 10^{-24}$ s^{-1}), provided that "R" nuclei may be found in a "fluid" state; in equilibrium, however, such is not possible due to the trapping in the metallic microfields. It has been remarked[4] that key factors in realizing "observable" fusion rates in MH should be sought in feasibility of achieving non-equilibrium "fluidlike" situations without effectively raising "temperatures" for the reacting nuclei.

The nuclear reactions in the PM cases under present study[1] differ in an essential way from those in the MH cases, in that the reacting nuclei are in *metallized, fluid* states where a substantial enhancement of the reaction rate due to the many-particle processes is expected as in the SN cases. Combination of Eq. (5) with the estimates of Eq. (7) shows in Table I that $d(p, \gamma)^3He$ and $^7Li(p,\alpha)^4He$ reactions can take place at a power-producing level on the order of a few kW/cm^3 if such a material is brought into a liquid-metallic state under an ultrahigh pressure on the order of 10 Mbar at a mass density of 3-7 g/cm^3 and a temperature of 500-700 K, slightly above the estimated melting conditions for hydrogen. These ranges of the physical conditions may be accessible through extensions of the current ultrahigh-pressure metal technologies (see, *e.g.*, refs. 12 and 13).

1 S. Ichimaru, J. Phys. Soc. Jpn **60**, 1437 (1991).
2 E.E. Salpeter and H.M. Van Horn, Ap. J. **155**, 183 (1969).
3 S. Ogata, H. Iyetomi, and S. Ichimaru, Ap. J. **372**, 259 (1991).
4 S. Ichimaru, S. Ogata, and A. Nakano, J. Phys. Soc. Jpn **59**, 3904 (1990).
5 S. Ichimaru and S. Ogata, Ap. J. **374**, 647 (1991).
6 A.G.W. Cameron, Ap. J. **130**, 916 (1959).
7 S. Ichimaru, Rev. Mod. Phys. **54**, 1017 (1982).
8 B. Widom, J. Chem. Phys. **39**, 2808 (1963).
9 H.E. DeWitt, H.C. Graboske, and M.C. Cooper, Ap. J. **181**, 439 (1973).
10 A. Alastuey and B. Jancovici, Ap. J. **226**, 1034 (1978).
11 S. Tanaka and S. Ichimaru, J. Phys. Soc. Jpn **53**, 2039 (1984).
12 W.J. Nellis *et al.*, Phys. Rev. Lett. **60**, 1414 (1988).
13 H.K. Mao, R.J. Hemley, and M. Hanfland, Phys. Rev. Lett. **65**, 464 (1990).

TABLE I PLASMA PARAMETERS, NUCLEAR REACTIONS, AND ENHANCEMENT

Assumed or calculated quantities	SN	SI	MH	PM	PM
Matter	C	H	Pd-D	D-H	Li-H
$\rho_m(g/cm^3)$	5×10^{9}	1×10^{2}	12.4	3.9	6.8
T(K)	1×10^{8}	1.5×10^{7}	300	600	550
Reactions	^{12}C-^{12}C	p-p	d-d	p-d	p-^{7}Li
S_{ij} (keV barn)	8.8×10^{19}	3×10^{-22}	106	2.5×10^{-4}	10^{2}
E_G (keV)	7.78×10^{5}	50	80	67	787
r_{ij}^* (10^{-13}cm)	6.7×10^{-2}	29	18	22	5.5
R_G (s^{-1})	1.3×10^{-44}	3.5×10^{-18}	--	--	--
(PLASMA EFFECTS)					
n_i (cm^{-3})	2.5×10^{32}	6.0×10^{25}	6.2×10^{22}	7.8×10^{23}	5.1×10^{23}
a_{ij} (10^{-8}cm)	1×10^{-3}	0.16	1.56	0.54	0.62
$\Gamma_{ij} \equiv \frac{Z_i Z_j e^2}{a_j T}$	61	0.07	285	520	492
$\Lambda_{ij} \equiv \frac{h}{a_j \sqrt{2 \mu_{ij} T}}$	0.203	0.011	0.235	0.458	0.362
$\Theta \equiv T/E_F$	1.8×10^{-4}	2.3	9.1×10^{-4}	1.1×10^{-3}	1.3×10^{-3}
D_S (10^{-8}cm)	3.2×10^{-3}	0.36	0.20	0.36	8.7×10^{-2}
$\Gamma_{ij}^s = \Gamma_{ij} \exp\left(-\frac{a_j}{D_S}\right)$	45	0.04	25.5	104	82
R_S (s^{-1})	--	--	1.6×10^{-36}	3.6×10^{-53}	1.2×10^{-46}
A_{ij}	5.0×10^{24}	1	2.9×10^{12}	3.9×10^{44}	4.1×10^{37}
R_{ij} (s^{-1})	6.8×10^{-20}	3.5×10^{-18}	4.6×10^{-24}	1.4×10^{-8}	4.5×10^{-9}
POWER (W/cm^3)	12	9.5×10^{-4}	3.7×10^{-13}	6.9×10^{3}	6.3×10^{3}

LIQUID METALLIC HYDROGEN: EQUATION OF STATE, TRANSPORT, AND IMPURITY IONIZATION

Setsuo Ichimaru
Department of Physics, University of Tokyo
Bunkyo, Tokyo 113, Japan

Strong interparticle correlations in hydrogen plasmas near metal-insulator transitions have been analyzed[1] through an integral equation approach, which adopts the hypernetted-chain (HNC) approximation[2] for the classical ion-ion correlation and the modified-convolution approximation (MCA) for the quantum-mechanical electron-electron and electron-ion correlations, at 48 parametric combinations (Fig. 1) between the Coulomb coupling parameter and the degeneracy parameter,

$$\Gamma \equiv \frac{e^2}{a k_B T}, \qquad \Theta \equiv \frac{k_B T}{E_F}, \tag{1}$$

where $a = (3/4\pi n)^{1/3}$ is the Wigner-Seitz radius. The results have clearly revealed the emergence of "*incipient Rydberg states* (IRS)" for the e-i correlations even in the metallic phase near the metal-insulator boundaries; the IRS acts significantly to modify the

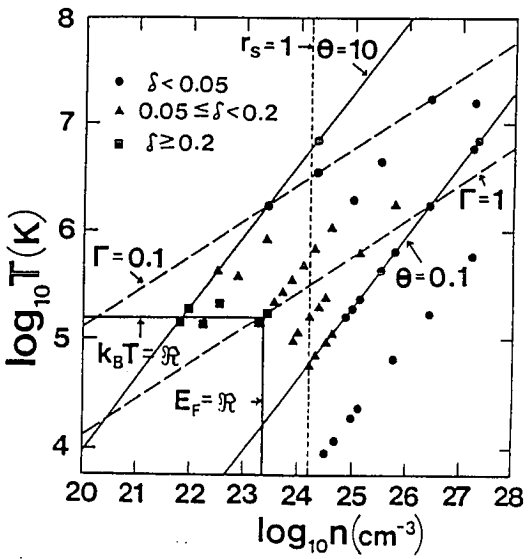

Fig. 1 Various parameters for liquid metallic hydrogen.

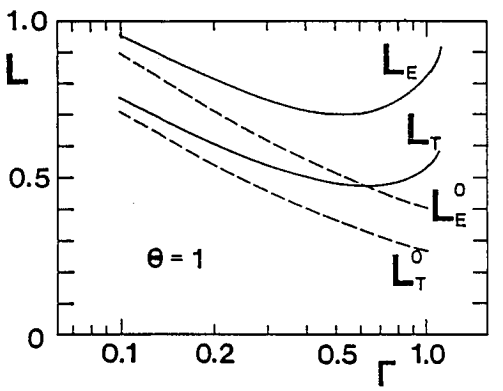

Fig. 2 Generalized Coulomb logarithms for the electric and thermal resistivities [see Eq. (6)].

equation of state (Fig. 1) and to enhance the rates of electron scattering (Fig. 2). In Fig. 2, the dased lines represent the results[3] of a theory in which the electron-ion scattering is treated in the Born approximation (*i.e.*, without the IRS). In Fig. 1, δ denotes a relative departure between the calculated interaction energy with and without the IRS: $\mathcal{R}$ = 13.6 eV.

The IRS may be characterized by the parameter,

$$x_b = \left\{ r_s \tanh\left[\hbar \left(\frac{2\pi}{mT} \right)^{1/2} n^{1/3} \right] \right\}^{1/2}, \qquad (2)$$

where r_s denotes a in units of the Bohr radius a_B. The quantity in the square bracket refers to a ratio between the thermal de Broglie wavelength, $\lambda_T \equiv \hbar(2\pi/mT)^{1/2}$, and a. Let us note that $\Delta p(r) = (me^2/r)^{1/2}$ measures the increment of momentum transferred at a Coulomb scattering with distance r. In a quantum limit where $a << \lambda_T$, Eq. (2) implies $x_b = r_s^{1/2} \sim \Delta p(a)/(\hbar/a)$, a ratio between characteristic momentum in an IRS and that in a free state. In a classical limit where $a >> \lambda_T$, one finds $x_b \sim \Delta p(\lambda_T)/(\hbar/\lambda_T)$, with implication similar to the above. Consequently we introduce $X = x_b/(1 + x_b)$, meaning a fraction of electrons in the IRS.

In such an IRS model, the normalized interaction energy $u_{ex} = U_{int}/nT$ may be formulated in the following way: Let $u_{ex} = u_{ee} + u_{ii} + u_{ei}$, and set an electronic screening function as

$$s(r) = A \exp(-K_s r) + X(B + CK_b r) \exp(-K_b r) \qquad (3)$$

with $s(0) = 1$. The e-i , e-e, and i-i interaction energies are then calculated as

$$u_{ei} = -(1 - X) e^2 K_s / k_B T - X e^2 K_b / k_B T , \qquad (4)$$

$$u_{ee} = u_{STLS}(\Gamma, \Theta), \qquad u_{ii} = u_{OCP}(\Gamma_s). \qquad (5)$$

Here $u_{STLS}(\Gamma, \Theta)$ and $u_{OCP}(\Gamma)$ are the STLS[2,4] interaction energy for the electrons and that for the classical one-component plasmas;[2] $\Gamma_s = \Gamma s(a)$.

The generalized Coulomb logarithms defined by

$$\rho_E = 4\sqrt{\frac{2\pi}{3}} \frac{\Gamma^{3/2}}{\omega_p} L_E(\Gamma, \Theta), \quad \rho_T = \frac{52\sqrt{6\pi}}{75} \frac{\Gamma^{3/2}}{\omega_p} \frac{T}{e^2} L_T(\Gamma, \Theta) \qquad (6)$$

may likewise be expressed in simple formulas as

$$L_E(\Gamma, \Theta) = \frac{5}{9} \frac{\ln\left[1 + (3/4)(C\zeta)^{-9/10} \right]}{1 - 0.376 x_b^2},$$

$$L_T(\Gamma, \Theta) = \frac{5}{9} \frac{\ln\left[1 + 0.5845 \times (3/4)(C\zeta)^{-9/10} \right]}{1 - 0.376 x_b^2}, \qquad (7)$$

where $C = 3.562\cdots$ and $\zeta = (3/2)(4/9\pi)^{2/3}\Gamma/\Theta$. In a weak coupling limit $\zeta << 1$, Eqs. (7) reproduce the Kivelson-DuBois result[5]; in the limit of strong Fermi degeneracy $\Theta << 1$, the usual Wiedemann-Frantz relation is satisfied; Eqs. (7) appear to suggest a divergence

(metal-insulator transition) at $x_b \approx 1.63$; quantitative accuracy of this prediction remains to be seen. We expect the opacities for liquid metallic hydrogen likewise be affected considerably by the presence of those IRS.

Table I compares between the theoretical[1] and the IRS-model values for the normalized interaction energy $u_{ex} = U_{int}/nT$, and the generalized Coulomb logarithms at 16 selected combinations of Γ and Θ.

The strong electron-ion coupling in the liquid metallic hydrogen affects in a number of ways to influence the degrees of ionization for the "impurity" atoms immersed in it: the effects include (a) equation of state for the hydrogen plasma; (b) shifts (shallowing) of the impulity atomic levels; (c) interaction between impurity-atoms and hydrogen plasma. Solutions to these problems bear important consequences to opacities, internal structures, and evolution in various stellar objects, including the giant planets, the Sun, and the brown dwarfs.

Relative atomic population for the j-th stage of ionization in

$$A^{j+} = A^{(j+1)+} + e^- , \tag{8}$$

may be determined from the sequential equations

$$\frac{P_j}{P_{j+1}} = \exp\left\{ \frac{\mu_{e0} + \mu_{XC} + \left(\mu_{j+1}^{AP} - \mu_j^{AP}\right) + \left(E_{j+1}^{B} - E_j^{B}\right)}{T} \right\} \tag{9}$$

with $\sum_j P_j = 1$.

Here μ_{e0}, μ_{XC}, μ_j^{AP}, and E_j^B are, respectively, the chemical potentials of ideal-gas electron, exchange-correlation electron, atom-plasma interaction, and the binding energy of a j-th stage atom. Acounting for those strong-coupling effects mentioned above, we calculate and discuss on the population numbers for He impurities in giant planets and the Sun, and for the Fe impurities in the Sun and a brown dwarf.

1 S. Tanaka, X.-Z. Yan, and S. Ichimaru, Phys. Rev. A **41**, 5616 (1990).
2 S. Ichimaru, H. Iyetomi, and S. Tanaka, Phys. Rep. **149**, 91 (1987).
3 S. Tanaka and S. Ichimaru, Phys. Rev. A **32**, 3756 (1985); S. Ichimaru and S. Tanaka, Phys. Rev. A **32**, 1790 (1985).
4 K.S. Singwi et al., Phys. Rev. **176**, 589 (1968).
5 M.G. Kivelson and D.F. DuBois, Phys. Fluids **7**, 1578 (1964).

TABLE I THE NORMALIZED INTERACTION ENERGY AND THE GENERALIZED COULOMB LOGARITHMS. The numbers in the parentheses are the IRS-model values.

Γ	Θ	$-u_{ex}$	L_E	L_T
0.05	10	0.027	2.732	2.363
		(0.025)	(2.630)	(2.298)
0.1	10	0.076	2.710	2.256
		(0.072)	(2.602)	(2.223)
0.2	10	0.218	3.295	2.557
		(0.237)	(3.175)	(2.637)
0.3	10	0.459	5.250	3.784
		(0.498)	(5.277)	(4.294)
0.1	5	0.750	2.097	1.725
		(0.697)	(2.602)	(2.223)
0.3	5	0.391	2.506	1.853
		(0.396)	(2.242)	(1.751)
0.5	5	1.095	5.002	3.384
		(0.991)	(5.158)	(3.884)
0.1	1	0.076	0.9560	0.7507
		(0.081)	(0.9781)	(0.7365)
0.4	1	0.491	0.7184	0.5024
		(0.486)	(0.5747)	(0.3880)
0.7	1	1.081	0.7214	0.4767
		(1.060)	(0.5108)	(0.3315)
1.0	1	1.882	0.8273	0.5301
		(1.822)	(0.5528)	(0.3511)
1.0	0.1	1.166	0.03679	0.02259
		(1.181)	(0.03903)	(0.02312)
3.0	0.1	4.289	0.02696	0.01614
		(4.250)	(0.01742)	(0.01024)
5.0	0.1	8.060	0.02612	0.01551
		(8.056)	(0.01341)	(0.00786)
10.0	0.01	13.290	0.0005776	0.0003377
		(13.274)	(0.0006390)	(0.0003736)
30.0	0.01	44.249	0.0004450	0.0002580
		(44.648)	(0.0002431)	(0.0001635)

NEUTRINO ENERGY LOSS IN DENSE HIGH-TEMPERATURE STARS

NAOKI ITOH

Department of Physics, Sophia University,
7-1, Kioi-cho, Chiyoda-ku, Tokyo 102 Japan

I. INTRODUCTION

Neutrino energy loss plays an essential role in the late stages of stellar evolution. In the present talk I will report on the four main neutrino energy loss processes. They are pair,photo-,plasma,and bremsstrahlung neutrino processes.

II. PAIR NEUTRINO PROCESS

The energy loss rate due to the pair neutrino process is expressed as (Munakata, Kohyama, and Itoh 1985; Itoh et al. 1989)

$$\begin{aligned} Q_{pair} &= \frac{1}{2}\left[(C_V^2 + C_A^2) + n(C_V'^2 + C_A'^2)\right] Q_{pair}^{+} \\ &+ \frac{1}{2}\left[(C_V^2 - C_A^2) + n(C_V'^2 - C_A'^2)\right] Q_{pair}^{-}, \qquad (1) \\ C_V &= \frac{1}{2} + 2\sin^2\theta_W,\ C_A = \frac{1}{2}, \qquad (2) \\ C_V' &= 1 - C_V,\ C_A' = 1 - C_A, \qquad (3) \\ \sin^2\theta_W &= 0.23, \qquad (4) \end{aligned}$$

where θ_W is the Weinberg angle and n is the number of the neutrino flavors other than the electron neutruno whose masses can be neglected compared with $k_B T$. At high temperatures($T > 10^9 K$), the energy loss rate due to the pair neutrino process is independent of the density and dominates over the other processes.

III. PHOTONEUTRINO PROCESS

The energy loss rate per unit volume per unit time due to the photoneutrino process is expressed as

$$\begin{aligned} Q_{photo} &= \frac{1}{2}\left[(C_V^2 + C_A^2) + n(C_V'^2 + C_A'^2)\right] Q_{photo}^{+} \\ &- \frac{1}{2}\left[(C_V^2 - C_A^2) + n(C_V'^2 - C_A'^2)\right] Q_{photo}^{-}, \end{aligned} \tag{5}$$

The photoneutrino process is dominant at relatively low densities and intermediate temperatures.

IV. PLASMA NEUTRINO PROCESS

The energy loss rate due to the plasma neutrino process is written as

$$Q_{plasma} = (C_V^2 + nC_V'^2) Q_V. \tag{6}$$

The expression for Q_V has been given by Beaudet, Petrosian, and Salpeter (1967) and also by Kohyama, Itoh, and Munakata (1986). The plasma neutrino process is dominant at high densities and intermediate temperatures.

V. BREMSSTRAHLUNG NEUTRINO PROCESS

The calculation of the bremsstiblung neutrino energy loss rate based on the Weinberg-Salam theory which takes the ionic correlation fully into account has been reported by Itoh and Kohyama (1983), Itoh et al. (1984 a,b,c). The bremsstrablung neutrino process is dominant at high densities and relatively low temperatures.

VI. COMPARISON OF VARIOUS NEUTRINO PROCESSES

In Figures 1-4 we show the contributions of the various neutrino processes for the case of $\sin^2\theta_W = 0.23, n = 2$, and ^{56}Fe matter corresponding to the temperatures $T = 10^7, 10^8, 10^9, 10^{10}$,and $10^{11} K$. In Figure 5 we show the most dominant neutrino process for a given density and temperature for the case of $n = 2$ and ^{56}Fe matter.

FIG.1

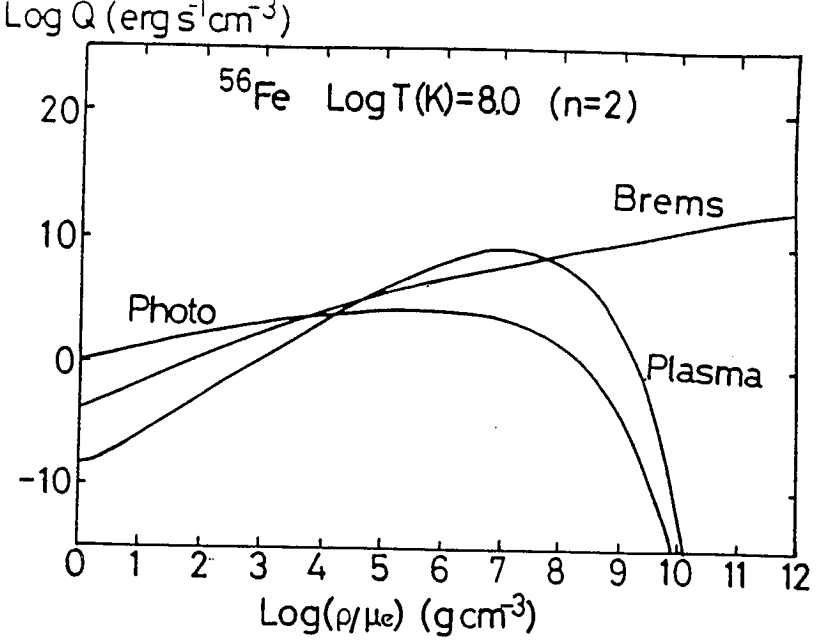

FIG.2

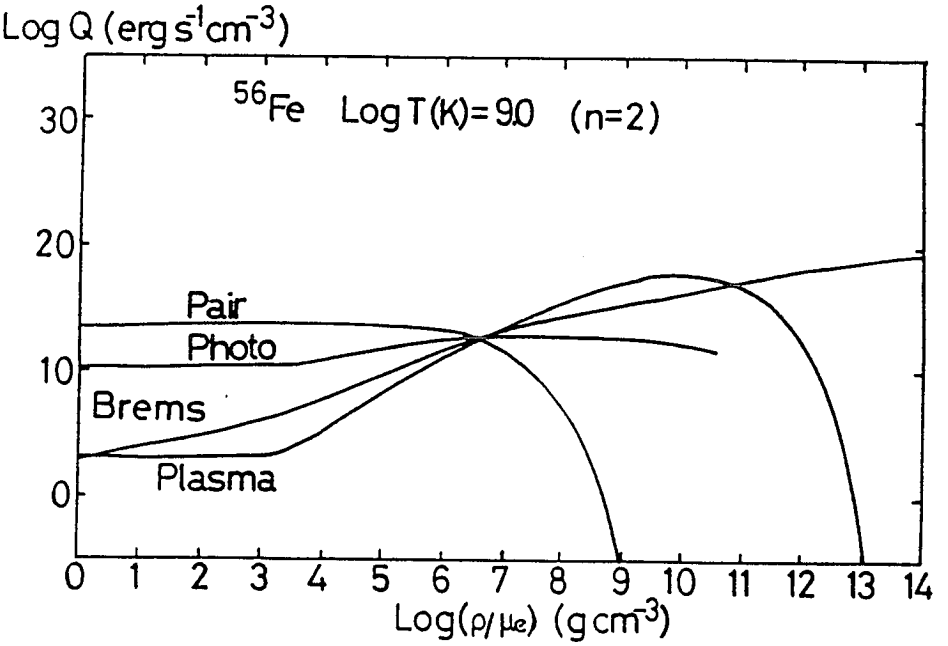

FIG.3

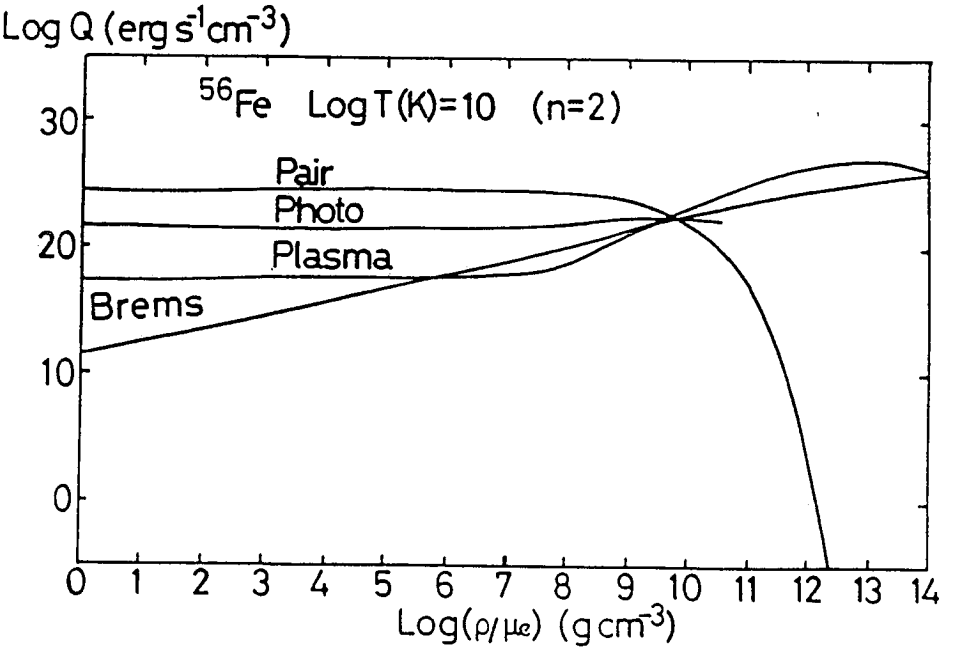

FIG.4

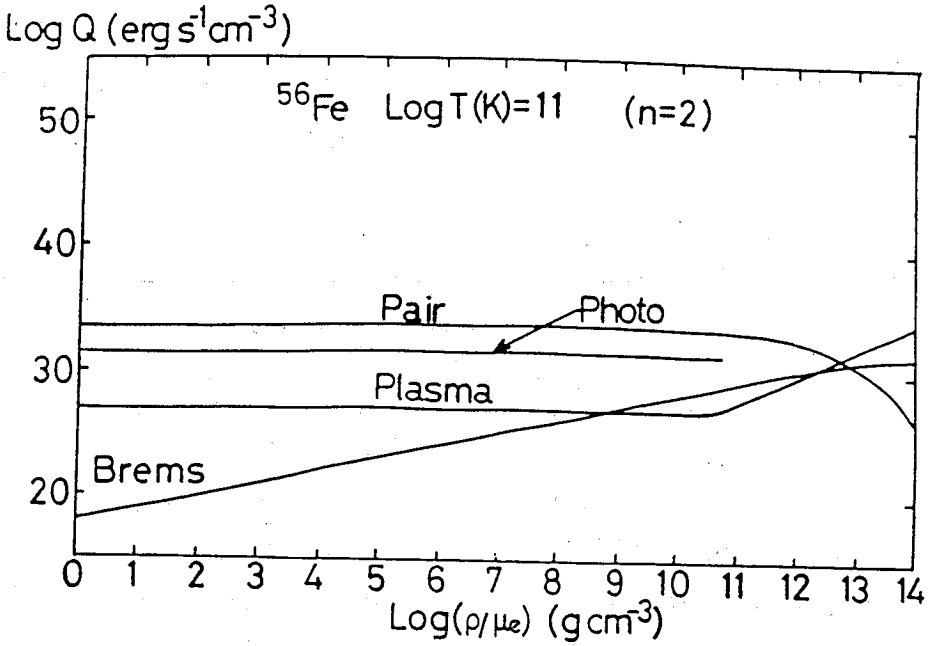

FIG.5

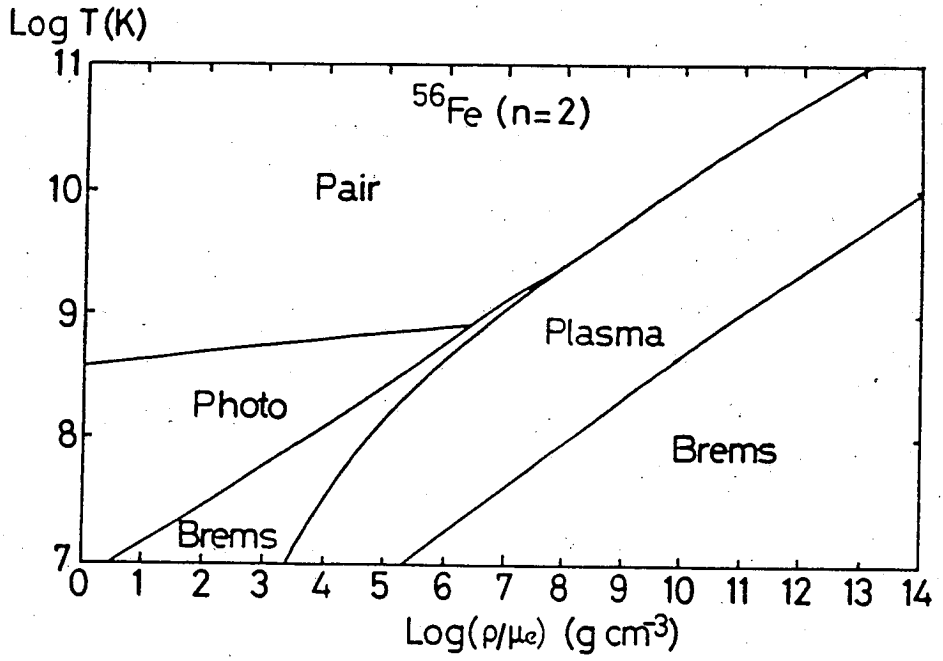

REFERENCES

Beaudet,G,Petrosian,V,and Salpeter,E.E.1967,Ap.J.,**150**,979.

Itoh,N.,Adachi,T.,Nakagawa,M.,Kohyama,Y.,and Munakata,H.,Ap.J., **339**,354.

Itoh,N.,and Kohyama,Y. 1983,Ap.J.,**275**,858.

Itoh,N.,Kohyama,Y.,Matsumoto,N.,and Seki,M.1984b,Ap.J.,**280**,787.

Itoh,N.,Kohyama,Y.,Matsumoto,N.,and Seki,M.1984c,Ap.J.,**285**,304.

Itoh,N.,Matsumoto,N.,Seki,M.,and Kohyama,Y.1984a,Ap.J.,**279**,413.

Kohyama,Y.,Itoh,N.,and Munakata,H. 1986,Ap.J.,**310**,815.

Munakata,H.,Kohyama,Y.,and Itoh,N. 1985,Ap.J.,**296**,197.

FREEZING TRANSITIONS AND PHASE SEPARATIONS IN DENSE MULTI-IONIC PLASMAS

Hiroshi Iyetomi, Shuji Ogata and Setsuo Ichimaru

Department of Physics, University of Tokyo
Bunkyo-ku, Tokyo 113, Japan

Dense plasmas with many ionic species are encountered in the interiors of astrophysical objects such as heavy planets and white dwarfs.[1,2] Freezing transitions incidentally take place in the plasmas on cooling and/or gravitational contraction of the stars. The multiplicity of ionic species also bring about novel issues associated with the mixing properties such as a limited solubility between ions of unlike species and a possible formation of an eutectic alloy. Such a possibility of phase transitions in dense plasmas critically controls the physical properties of stellar matter through the equation of state, the elementary processes including nuclear reactions, and the transport coefficients. Precise knowledge on these issues is thereby indispensable to understand quantitatively or even qualitatively the internal structures and the evolutional processes of dense stars .

Since the phase properties of dense plasmas so sensitively depends on the assessment of the thermodynamic functions, we have to take proper account of various kinds of physical effects. In this talk we present the theoretical progresses that we have recently made in dealing with strong Coulomb correlations and quantum effects of ions, together with a study on the miscibility problem in carbon-iron mixtures under the internal conditions of white dwarfs.

1. Bridge Function and Improvement on the HNC Approximation in the Classical OCP

The classical one-component plasma (OCP) consisting of identical ions (charge Ze) in a uniform neutralizing background is a prototype model for the present study.[1] The OCP with temperature T and number density n is uniquely characterized by the parameter Γ defined as

$$\Gamma = \frac{(Ze)^2/a}{k_B T}, \qquad (1)$$

with $a = (3/4\pi n)^{1/3}$.

Recently we have succeeded in extracting the bridge function B(r) in the OCP fluid from Monte Carlo (MC) simulations almost within the original statistical uncertainty. The strong correlations at short distances are represented by B(r) and setting B(r) = 0 gives the hypernetted-chain (HNC) approximation.[3] The short-range expansion formula[4,5] for the screening potential and the sum rules[6] for the static structure factor were effectively used to extend the finite-range MC data. We have also provided an improved hypernetted-chain (IHNC) scheme by making an analytic formula for the extracted results:

$$\frac{B(r)}{\Gamma} = (- b_0 + b_2x^4 + b_3x^6 + b_4x^8) \exp\left(- \frac{b_1}{b_0} x^2\right), \quad (2)$$

with x = r/a and

$$b_0 = -0.0612 + 0.0629 \ln \Gamma$$
$$b_1 = -0.0717 + 0.0910 \ln \Gamma$$
$$b_2 = 0.498 - 0.280 \ln \Gamma + 0.0294 (\ln \Gamma)^2$$
$$b_3 = - 0.412 + 0.219 \ln \Gamma - 0.0251 (\ln \Gamma)^2$$
$$b_4 = 0.0988 - 0.0534 \ln \Gamma + 0.00682 (\ln \Gamma)^2. \quad (3)$$

Figure 1 summarizes the extracted results for B(r) along with the fitting (2) and confirms the accuracy of the IHNC scheme from various points of view.

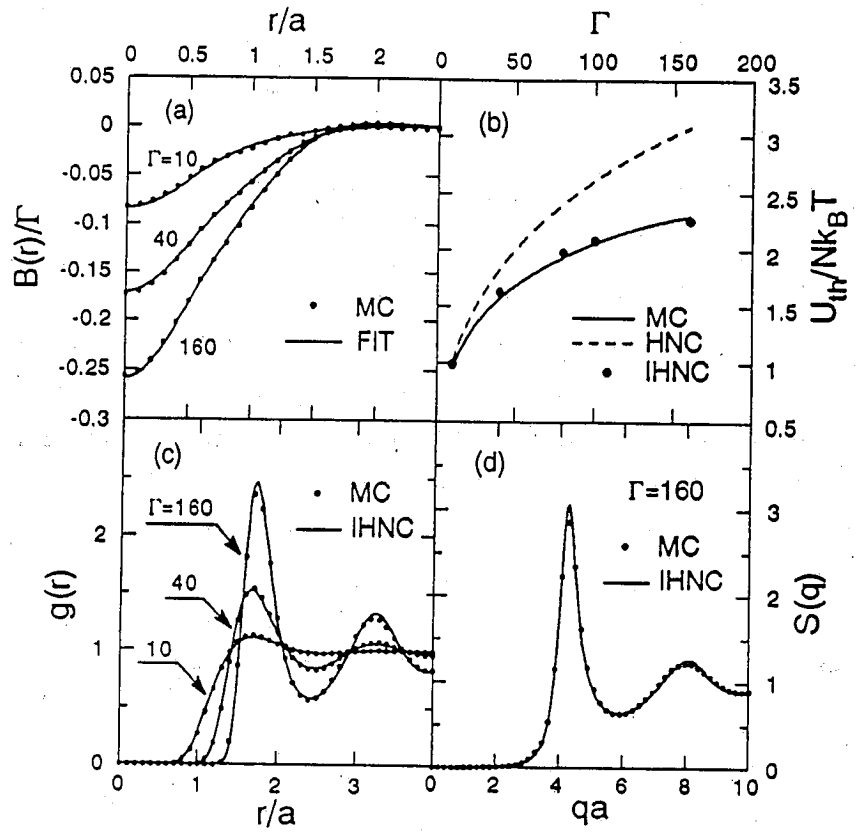

Fig. 1 Detailed analysis of the bridge function B(r) based on the MC simulations and the IHNC scheme in the classical OCP. Frame(a): B(r) extracted from the MC data with the fitted results; Frame(b): the thermal fraction in the excess internal energy; Frame(c): the radial-distribution function; Frame(d): the static structure factor.

2. Quantum MC Simulations on the OCP Solid

We have carried out quantum MC simulations on the solid OCP to study quantum effects on the freezing. Let us introduce an additional parameter characterizing the quantum nature of the OCP,

$$Y = \hbar\omega_p/\sqrt{3}k_BT, \quad (4)$$

where ω_p is the plasma frequency. The partition function was represented in a form of the Feynman path-integral and sampled using a semiclassical reference system with quantum fluctuations generated according to the ion-sphere model. The free energy of the solid

OCP was calculated over a wide range of T and n with 128 MC particles. Its accuracy was assured by comparing with the semiclassical (SCL) expansion results[7] and the ground-state (GS) results[8] of the zero-temperature solid (See Fig.2). The free energy was then decomposed into the harmonic (HM) and anharmonic(AHM) contributions, each of which was fitted to an analytic form:

$$\frac{F_{harm}}{Nk_BT} = 3\ln\left[2\sinh\left(\frac{Y}{2}f(Y)\right)\right]; \quad f(Y) = \frac{0.7543+0.09245Y^2+0.003386Y^4}{1+0.1046Y^2+0.003823Y^4}, \tag{5}$$

and

$$\frac{F_{anh}}{Nk_BT} = \Gamma\frac{P(\xi) + 0.002P(\xi)Y^2 + R(\xi)Y^4}{1 + 0.002Y^2 + Q(\xi)Y^4}, \tag{6}$$

with

$$\xi = \Gamma\tanh(\alpha/Y) \text{ with } \alpha = 8,\ P(\xi) = -\frac{g}{2\xi^3} \text{ with } g = 3225,$$

$$Q(\xi) = \frac{1.2993\xi + 61.252}{80(0.365\alpha^2\xi - g/2)},\ R(\xi) = -\frac{0.365\alpha^2}{\xi^2}Q(\xi). \tag{7}$$

These formulae recover both the semiclassical and zero-temperature results.

As an application of (5) and (6), we calculated the freezing curves in the carbon OCP as shown in Fig. 2, where the quantum corrections to the free energy of the classical OCP fluid are systematically included up to the fourth power of the Planck constant. The freezing condition in the classical OCP is given by Γ=180. The calculations reflect the sensitive dependence of the transition curve on the treatment of the quantum properties of ions.

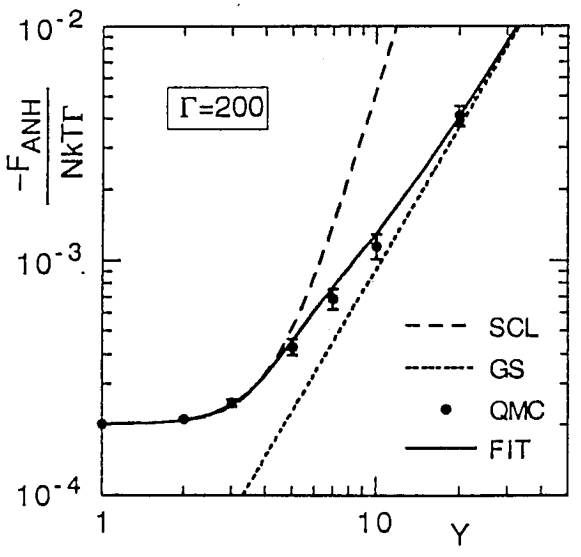

Fig. 2. Anharmonic contributions in the free energy of the solid OCP based on various schemes

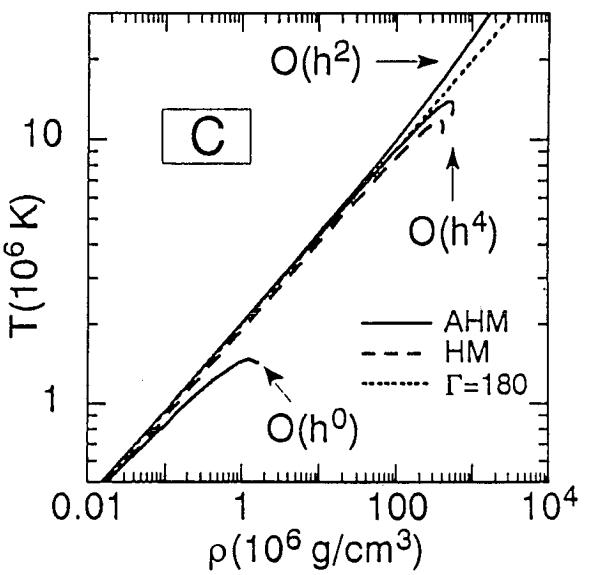

Fig. 3. Freezing curves in the carbon OCP in various schemes

3. Carbon-Iron Binary Ionic Mixtures

The miscibility of minor heavy elements (Ne, Fe, etc.) in C-O mixtures is of astrophysical interest in relation to the cooling of white dwarfs.[2] If the segregation of the minor elements happen, the gravitational energy is released to prolong the cooling time.

To obtain the equation of state for a fluid binary ionic mixture (BIM), we have generalized the IHNC scheme which has been developed in the OCP to multi-ionic cases using the ion-sphere scaling for length and energy. We have also extensively performed MC simulations for several BIM's. The accumulation of those MC data enabled us to make an analytical formula for the equation of state. Comparison with the MC data shows that the IHNC scheme improves the HNC results significantly. We note that the linear mixing (LM) law is satisfied with excellent accuracy (less than 0.15%) even for such an asymmetric BIM.

Taking a C-Fe mixture as an example, we have calculated the phase separation curves using the equations of states based on the MC, IHNC and LM schemes (See Fig. 4). The small difference of the order of 0.1% in the equations of state gives rise to the substantial change of the coexistence curve. Since the temperature range is comparable to that of the crystallization conditions ($T_C = 2\times10^6$ K for the C-OCP), however, an analysis with account for a possible freezing transition is required.

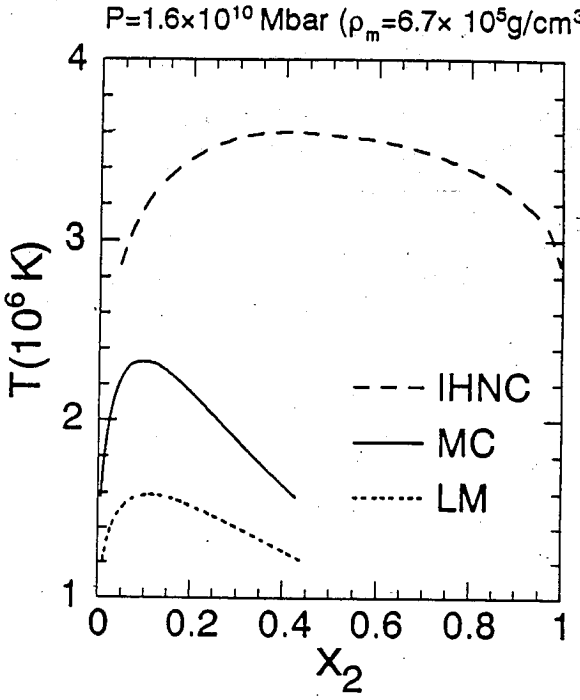

Fig. 4. Phase separation curves in the BIM with $Z_1 = 6$ and $Z_2 = 24$.

1. S. Ichiamru, H. Iyetomi and S. Tanaka, Phys. Rep. **149**, 91 (1987).
2. H.M. Van Horn, Science **252**, 384 (1991).
3. J.-P. Hansen and I.R. MaDonald, *Theory of Simple Liquids* (Academic Press, London, 1986).
4. B. Jancovici, J. Stat. Phys. **17**, 357 (1977).
5. S. Ogata, H. Iyetomi and S. Ichimaru, Astrophys. J. **372**, 259 (1991).
6. P. Vieillefosse and J.-P. Hansen, Phys. Rev. A **12**, 1106 (1975).
7. J.-P. Hansen and P. Vieillefosse, Phys. Lett. **53A**, 187 (1975).
8. W.J. Car, Jr., R.A. Coldwell-Horsfall and A.E. Fein, Phys. Rev. **124**, 747 (1961).

ANOMALOUS NUCLEAR EFFECTS IN DEUTERIDED SOLIDS: PRELIMINARY NEW RESULTS

Presented by Steven E. Jones
Department of Physics and Astronomy
Brigham Young University
Provo, UT 84604

Pursuant to our studies of possible nuclear reactions in deuterium-charged solids [1,2], we have searched for charged particles at Brigham Young University and for neutrons and gammas at Kamioka, Japan. We find evidence for very low-level nuclear reactions, excluding cosmic-ray effects. Geophysical implications will be considered.

1. C.D. Van Siclen and S.E. Jones, "Piezonuclear Fusion in Isotopic Hydrogen Molecules," J. Phys. G: Nuclear Phys. (1986) 12: 213-221 (1986).

2. S.E. Jones, E.P. Palmer, J.B. Czirr, D.L. Decker, G.L. Jensen, J.M. Thorne, S.F. Taylor and J. Rafelski, "Observation of Cold Nuclear Fusion in Condensed Matter," Nature 338: 737-740 (1989).

MODES IN GLUON AND QUARK GLUON PLASMAS

S.M. Mahajan

Institute for Fusion Studies
The University of Texas at Austin
Austin, Texas 78712

ABSTRACT

In nonablian gauge theories, the carriers of interaction (gluons) can directly interact with one another giving rise to a new dynamically interesting system; the gluon plasma. A study of this system is of interest to the problem of confinement of the quarks and gluons in hadrons as well as to the evolution of the early universe. We investigate two different kinds of gluon structures within the framework of SU(2) and SU(3) classical chromodynamics: 1) a collection of gluons which will produce a trap for the confinement of other gluons and quarks, a state which could be thought of as a nontrivial vacuum around which a quantum theory could be built and 2) the collection of gluon excitations about this nontrivial vacuum. Normal modes of the latter system are presented and it is shown that the dispersion relation is characteristic of a massive particle rather than the massless free gluon. This magnetic mass provides a clue to self-confinement of the gluons.

* * * * * * * * * *

Baryon Inhomogeneities and the Primordial Light-Element Abundances

Richard A. Matzner
Department of Physics
Center for Relativity
University of Texas at Austin

Abstract

Inhomogeneous cosmic nucleosynthesis with extremely high contrasts (up to $R = 10^4$) in baryon-number density is investigated. Because those models develop sharp structure at the boundaries between the high- and low-density regions, accurate results require a high resolution. Such high-resolution numerical simulations are carried out and it is found that inhomogeneity in a closure density ($\Omega_b = 1$) model cannot bring the ^4He yields down to fit observational constraints. Investigation of the detailed process dynamics shows that neutrons diffuse so rapidly during nucleosynthesis that they cannot effectively be separated from protons for long enough times to significantly suppress ^4He.

ELECTROCHEMISTRY AND CALORIMETRY OF THE D/Pd SYSTEM

By:

Michael C.H. McKubre
Francis L. Tanzella
Stuart I. Smedley
SRI International
Menlo Park, CA

and

Steven Crouch-Baker
Joseph Santucci
Electric Power Research Institute
Palo Alto, CA

Experiments have been performed in three basic categories in an attempt to explore reported anomalies in the deuterium/palladium system at very high loadings of D.

Electrochemical kinetic measurements have been performed in conjunction with measurements of bulk loading (D/Pd atomic ratio) to study the mechanisms and kinetics of deuterium ion discharge, adsorption and absorption at the palladium/electrolyte interface. This interface provides the gateway to absorption of hydrogen isotopes into the bulk metal phase. It is critical, therefore, to understand the elementary processes occurring at this interface and the role of impurity species, in order to reproducibly obtain high loading. By judicious control of the electrolyte composition, temperature and current density, it is possible to attain atomic ratio's inferred from the measured cathode resistance ratio, close to or exceeding 1.

A major effort of the experimental program has been the design and development of high accuracy, isothermal flow calorimeters capable of extended use. First Law calorimeters have been constructed with a conservative design capable of 0.1% accuracy at output powers up to 100W, and stable operation for periods of weeks or months Approximately 30 calorimeter experiments have been performed with durations extending from several hundred to several thousand hours, pressures from atmospheric to 10,000 psi D_2, and current densities typically 300-600 mA cm^{-2} but as high as 5 A cm^{-2}. All experiments have been performed with closed cells employing an internal recombiner or hydrogen anode to prevent pressure buildup. Calorimetry experiments performed with Pd electrodes that attain and maintain high loading are observed to exhibit heat output in excess of all known sources of integrated input energy.

A program of nuclear monitoring has been undertaken in conjunction with the electrochemical kinetic and calorimetric investigations. Experiments have been monitored for neutrons and gamma rays using multiple detectors. No attempt was made to develop a low level detection capability. No unambiguous observation of neutrons or gamma rays were made in ~ 30 experiments. Distilled samples of the initial and final electrolyte have been assayed for tritium in all experiments using a scintillation cocktail. Approximately 350 determinations have been made, including ~12 samples from cells in which excess heat has been observed. In no case was there clear evidence for tritium production.

DENSE CORE PLASMA IN AN INERTIAL ELECTROSTATIC CONFINEMENT DEVICE

George H. Miley
Fusion Studies Laboratory
Department of Nuclear Engineering
University of Illinois
Urbana, IL 61801

ABSTRACT

Inertial-Electrostatic Confinement (IEC) is an alternative approach to fusion power that potentially offers the ability to burn both D-T and advanced fuels, D-He^3, in a non-Maxwellian, high density core. Such a device would be attractive for a variety of compact high power density applications, e.g., space power [1].

The principle of IEC involves the confinement of a fusion plasma inside of one or more potential wells that are created at the center of a hollow spherical grid (cathode). This semi-transparent cathode attracts ions, generating a spherical ion "beam" that flows radially through the cathode and then converges at the center of the spherical volume, creating a space charge (potential well) there. Electrons are attracted toward the accumulated space charge (virtual anode) at the center. They, in turn, create a virtual cathode. This is very important since a virtual cathode (vs. a physical grid) is 100% transparent. Ions trapped inside this well oscillate back and forth until they fuse or up-scatter out of the well. These multiple wells with virtual anodes and cathodes, have been called "Poissors" following the original work by Farnsworth [2] and by Hirsch [3]. A brief description of the theory of IEC is given, followed by a discussion of recent experimental results.

Simulations of IEC experiments have been done using the XL-code, (written by D. Smithe, MRC) to solve Poisson's equation, self-consistently with the collisionless Vlasov equation, for different current species and parameters in spherical geometry.

The experimental results presented here are the first potential well measurements of an IEC-type device via a collimated proton detector.[4] They indicate that a ~15-kV virtual anode, at least one centimeter in radius, has formed in a spherical device with a cathode potential of 30 kV, and a current of 12 mA. Numerical analysis indicates D^+ densities on the order of 10^9 cm^{-3}, and D^+_2 densities on the order of 10^{10} cm^{-3}.

[1] G. MILEY, J. NADLER, T. HOCHBERG, Y. GU, O. BARNOUIN, and J. LOVBERG, "Inertial-Electrostatic Confinement: An Approach to Burning Advanced Fuels," Fusion Tech., 19, Part 2A, 840 (1991).
[2] P. T. FARNSWORTH, U. S. Patent #3,258,402 (1966).
[3] R. L. HIRSCH, "Inertial-Electrostatic Confinement of Ionized Fusion Gases," JAP, 38, 4522 (1967).
[4] J. NADLER, T. HOCHBERG, Y. GU, O. BARNOUIN, and G. MILEY, "Advantages of Inertial-Electrostatic Confinement Fusion," Proc. Sixth Intern. Conf. on Emerging Nuclear Energy Systems, Monterey, CA, June 16-21, 1991.

Effect of Radiative Processes on Radiation Transport

Katsunobu Nishihara

Institute of Laser Engineering, Osaka University
2-6 Yamada-oka, Suita, Osaka 565, Japan

When a gold foil is irradiated by an intense laser of the order of 10^{14} W / cm^2, more than a half of an absorbed energy is converted to soft x-ray. Radiation energy density is therefore very large near the surface and radiative processes of excitation and ionization can not be neglected. Effects of radiative processes on the ionization state and radiation spectrum are investigated. The results obtained by taking the radiative processes into account are compared with those by the conventional CRE (Collisional Radiative Equilibrium) model.

In a over dense region where electron density is greater than a laser critical density, the brightness temperature of the radiation becomes comparable to the electron temperature. It is thus shown that the radiative ionization rate from N-shell is bigger than the collisional ionization rate, and that the ionization state is approximated by the LTE model rather than the CRE model in the over dense region. However the ionization state in a under dense region can not be approximated by neither the LTE nor the CRE model.

The increase of the ionization from N-shell by the radiative processes results in the enhancement of the emission. The x-ray spectrum obtained is compared with the experiment.

Nonlinear AC Conductivity of Solid Density Plasma

K. Nishihara, H. Yasui, S. Kato and K. Mima

Institute of Laser Engineering, Osaka University
2-6 Yamada-oka, Suita, Osaka 565, Japan

The interaction of an intense ultrashort laser pulse with matter has recently attracted much interest. If a pulse duration of a laser light is so short that no significant hydrodynamic expansion of a matter takes place, the electric field of a laser interacts directly with a solid density matter. We evaluated the nonlinear high frequency conductivity of solid density plasmas and estimate absorption efficiency as a function of the intensity, both analytically, and using of 3d particle code "SCOPE".

Since ions are strongly coupled in such plasmas, the ion-ion correlation is described by the hypernetted-chain (HNC) equation. On the other hand, the electron-ion correlation is treated by the linear response theory. The quiver velocity and excursion length are finite in comparison with the electron thermal speed and shielding distance respectively.

In the 3d two component (electron and ion) particle code "SCOPE (Strongly COupled plasma ParticlE code)", short range forces are calculated by using a direct particle-particle summation over spatially localized forces and long-range forces by particle-in-cell method.

NUCLEAR REACTION RATES IN DENSE MULTI-IONIC STELLAR MATERIALS

Shuji Ogata,[†,‡] Setsuo Ichimaru,[†,‡] and Hugh M. Van Horn[‡]

[†]Department of Physics, University of Tokyo
Bunkyo-ku, Tokyo 113, Japan

[‡]Department of Physics and Astronomy, University of Rochester
Rochester, NY 14627-0011

Nuclear reaction rates between nuclei, i and j, are in general proportional to the contact probability, $g_{ij}(0)$, and are enhanced[1] by the many-body correlations between the reacting and the surrounding nuclei. Inside dense stars such as white dwarfs and neutron stars, ions (He, C, O,$\cdots$) are strongly coupled[2] since their Coulomb coupling parameters, $\Gamma \equiv$ (Coulomb energy)/(thermal energy) = 10–100; electrons are relativistically degenerate and may be regarded as a uniform negative-charge background for ions in the zero-th order approximation. The enhancement factors of the nuclear reaction rates due to strong coupling effects of ions for charge-ratio $Z_2/Z_1 \simeq 1$ are already calculated[3] based on $g_{ij}(r)$ accurately determined by the Monte Carlo (MC) simulation method. We extend the calculations to cases where $Z_2/Z_1 > 1$ and then evaluate the screening correction of electrons to the enhancement factors.

As an example of nuclear reactions in multi-ionic stellar materials, we consider the He (3α) reaction in He-C mixtures. Helium burning occurs in accreting white dwarfs and neutron stars in close binary systems, where it may play a key role in understanding the mechanisms of Type-I supernova (SNI) and X-ray bursts.[4,5] Based on newly performed MC simulations for binary-ionic mixtures (BIM) with $Z_2/Z_1 = 3$ and 5 for various combinations of $x = n_2/n$ (molar fraction of "2" ions) and various Coulomb coupling parameters, we calculate the enhancement factors and show their effects on the He ignition curves.

SCREENING POTENTIALS Screening effects of the surrounding nuclei on the reacting two ions are represented by the screening functions defined as

$$H_{ij}(r) = \frac{Z_i Z_j e^2}{r} + k_{\rm B} T \ln g_{ij}(r) \ . \tag{1}$$

For the one-component plasmas and for C-O BIMs ($Z_2/Z_1 = 4/3$), screening functions are known accurately through the MC simulations[3] and are parameterized to better

than 0.1% by Eq. 2 below, for the regime defined by $5 \lesssim \Gamma_{ij} \equiv \frac{2Z_iZ_j}{Z_i^{1/3}+Z_j^{1/3}}\Gamma_e \leq 180$, $\Gamma_e = e^2/a_e k_B T$, $a_e = (3/4\pi n_e)^{1/3}$ (n_e= density of background electrons):

$$\frac{H_{ij}(r)}{\Gamma_{ij}k_BT} = \begin{cases} A - B\frac{r}{a_{ij}} + \frac{a_{ij}}{r}\exp\left[C\sqrt{\frac{r}{a_{ij}}} - D\right], & \text{for } \frac{B}{2h_1} \leq \frac{r}{a_{ij}} < 2\,, \\ h_{ij}(0) - h_1\left(\frac{r}{a_{ij}}\right)^2, & \text{for } \frac{r}{a_{ij}} < \frac{B}{2h_1} \end{cases} \tag{2}$$

where

$$h_{ij}(0) = A - \frac{B^2}{4h_1}\,,\ h_1 = \frac{(Z_i^{1/3}+Z_j^{1/3})^3}{16(Z_i+Z_j)}\,,$$
$$A = 1.356 - 0.0213\ln\Gamma_{ij}\,,\ B = 0.456 - 0.0130\ln\Gamma_{ij}\,,$$
$$C = 9.29 + 0.79\ln\Gamma_{ij}\,,\ D = 14.83 + 1.31\ln\Gamma_{ij}\,.$$

Here $a_{ij} \equiv (a_i + a_j)/2$ and $a_i = Z_i^{1/3}a_e$ is the ion-sphere radius[2] for the ions with charge Z_i. The function $H_{ij}(r)/\Gamma_{ij}k_BT$ is independent of the molar fraction x and depends only weakly on Γ_{ij}. As Eq. 2 shows, $H_{ij}(r)/\Gamma_{ij}k_BT$ is a function of the scaled variable r/a_{ij}; that is, the ion-sphere scaling law applies with remarkable accuracy for BIMs with $1 \leq Z_2/Z_1 \leq 4/3$.

We have performed new MC simulations with $N = 1000$ test particles for BIMs with $(Z_1, Z_2) = (1, 3)$ for $\Gamma_e = \{10, 15, 20\}$ and $x = \{0.01, 0.05, 0.1, 0.2, 0.5\}$ and with $(Z_1, Z_2) = (1, 5)$ for $\Gamma_e = \{5, 7, 10\}$ and $x = \{0.01, 0.05, 0.1, 0.2, 0.5\}$. The total number of configurations was 7×10^6 for each case. Examples of the resulting screening functions are shown in Fig. 1: the MC results are shown by the small circles while the prediction of the ion-sphere scaling is given by the solid curves. Except for extreme cases, the ion-sphere scaling law applies exceptionally well; in the actual application to the 3α reaction, the slight difference in $H_{ij}(r)$ between the MC values and Eq. 2 influences the reaction rates by less than 10%. Only for the cases $x = 0.01$ with $(Z_1, Z_2) = (1, 5)$, can the deviation from Eq. 2 be seen clearly at short distances between ions "1" and "2".

THE 3α REACTION We apply the results for the screening potentials discussed in the previous section to the evaluation of the 3α reaction rates in He-C materials. With applications to model calclulations[4,5] of SNI and X-ray bursts in mind, we assume the density-temperature range to be given by $\rho_m(\mathrm{g/cm^3}) = 10^6$–$10^9$ and $T(\mathrm{K}) = 10^7$–10^8. In this range, the Coulomb coupling parameter between He ions is conveniently written as $\Gamma_{\mathrm{HeHe}} = 26.6\rho_8^{1/3}/T_7$.

The 3α reaction is known to take place in three steps[6]: (i) $^4\mathrm{He} + {}^4\mathrm{He} \leftrightarrow {}^8\mathrm{Be} - 0.092\mathrm{MeV}$, (ii) $^8\mathrm{Be} + {}^4\mathrm{He} \leftrightarrow {}^{12}\mathrm{C}^* - 0.278\mathrm{MeV}$, (iii) $^{12}\mathrm{C}^* \rightarrow {}^{12}\mathrm{C} + 7.644\mathrm{MeV}$, where the energy differences are from Refs. 7 and 8. It is interesting to compare the lifetime

of the unstable ^{8}Be with the thermal relaxation time of the ions. Since the half width is[7] $\gamma_{\rm Be} = 6.8$eV, the lifetime $\tau = \hbar/\gamma_{\rm Be} \sim 10^{-16}$s. Assuming the thermalization cross section[2] to be $\sigma \sim \pi a^2$, where a is the mean separation of ions, the thermal relaxation time of the ions is $\tau_{\rm rel} \sim \sqrt{\Gamma}\omega_p^{-1} \sim 10^{-18}\rho_8^{-1/3}T_7^{-1/2}$(s). Therefore we have $\tau_{\rm rel} \ll \tau$ in the density-temperature range we are considering. Screening effects of the surrounding ions on the reacting ^{8}Be and ^{4}He ions may thus be evaluated by considering Be-He BIMs in thermal equilibrium. The 3α reaction rates are thus proportional to the product of the contact probabilities, i.e., $g_{\rm HeHe}(0)g_{\rm BeHe}(0)$; that is, it is *not* necessary to consider the *three*-particle probabilities for this case.

Solving the Schrödinger equations numerically with the effective potential $W_{ij}(r) = Z_iZ_je^2/r - H_{ij}(r)$ appropriate for S-wave scattering, we obtain the enhancement factor for each reaction as $g_{ij}(0)/g_{ij}(0;H_{ij}=0) = |\Psi_{ij}(0)|^2/|\Psi_{ij}(0;H_{ij}=0)|^2$. The resulting enhancement factor for the overall 3α rate is given by

$$[\text{Enhancement factor}] = \exp(Q_{\rm HeHe} + Q_{\rm BeHe})A^e_{\rm HeHe}A^e_{\rm BeHe}\ . \tag{3}$$

Here

$$Q_{ij} = \frac{H_{ij}(0)}{k_{\rm B}T} - \frac{5}{32}\Gamma_{ij}\left(\frac{3\Gamma_{ij}}{\tau_{ij}}\right)^2 \times\left\{1+(1.1858-0.2472\ln\Gamma_{ij})\left(\frac{3\Gamma_{ij}}{\tau_{ij}}\right)-0.07009\left(\frac{3\Gamma_{ij}}{\tau_{ij}}\right)^2\right\} \tag{4}$$

where $\tau_{ij} = (27\pi^2Z_i^2Z_j^2e^4\mu_{ij}/2k_{\rm B}T\hbar^2)^{1/3}$, μ_{ij} is the reduced mass, and A^e_{ij} is the screening correction due to electrons, the formula for which is explicitly presented in Ref. 9.

He IGNITION CURVES In Fig. 2, we show the ignition curves[4,5] for pure He material ($x = 0$). These are defined as the loci where the timescale for the temperature rise due to nuclear burning, $\Delta T_{\rm He} \equiv C_pT/\epsilon_{\rm He}$, equals 10^6 years. For the 3α energy generation rate without many-body effects, we adopt the formulas given by Nomoto et al.[5] The dotted curve corresponds to the case where only the classical term, $H_{ij}(0)/k_{\rm B}T$, in Eq. 4 is included; for the dashed curve, the lowest-order quantum correction term, $-\frac{5}{32}\Gamma_{ij}(3\Gamma_{ij}/\tau_{ij})^2$, is included in addition to the classical term; and the dot-dashed curve corresponds to Eq. 4. The solid curve shows the case where screening corrections due to electrons are included.

ACKNOWLEDGMENTS This research was supported in part by Grants-in-Aid for Scientific Research provided by the Ministry of Education, Science, and Culture, and in part by the U. S. National Science Foundation under grant INT90-16293 through the University of Rochester. We are grateful to Dr. H. Iyetomi for useful discussions.

REFERENCES

[1] E. E. Salpeter and H. M. Van Horn, Ap. J. **155**, 183 (1969).

[2] See e.g., S. Ichimaru, *Plasma Physics:* An Introduction to Statistical Physics of Charged Particles (Benjamin/Cummings, Menlo Park, CA, 1986).

[3] S. Ogata, H. Iyetomi, and S. Ichimaru, Ap. J. **372**, 259 (1991).

[4] K. Nomoto, Ap. J. **253**, 798 (1982).

[5] K. Nomoto, As. Ap. **149**, 239 (1985).

[6] E. E. Salpeter, Phys. Rev. **88**, 547 (1952).

[7] F. Ajzenberg-Selove and C. L. Busch, Nucl. Phys. A **336**, 1 (1980).

[8] F. Ajzenberg-Selove, Nucl. Phys. A **413**, 1 (1984).

[9] S. Ichimaru and S. Ogata, Ap. J. **374**, 647 (1991).

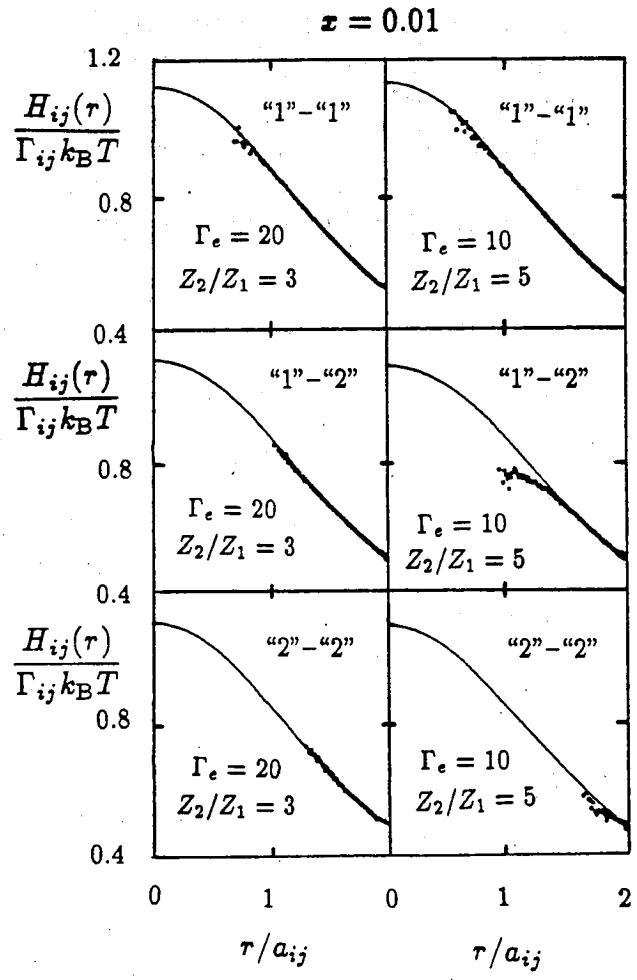

Fig. 1 Screening potentials.

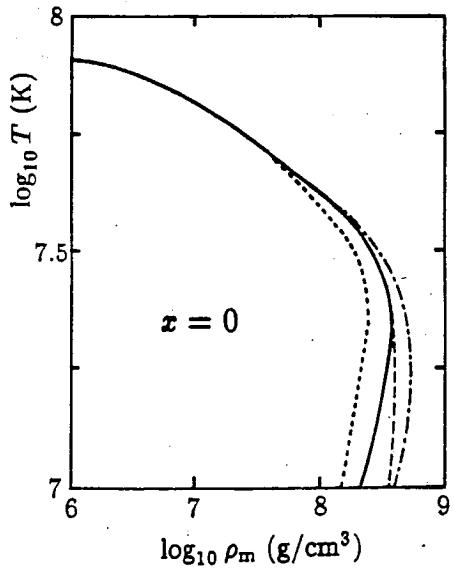

Fig. 2 He ignition curves.

Opacity in Stellar Plasmas

Forrest J. Rogers and Carlos A. Iglesias
Lawence Livermore National Laboratory
Livermore, Ca 94550

A review of the equation of state and atomic physics basis of the OPAL opacity code will be given. Some comparisons will be made with the Mihalas, Hummer, and Dappen (MHD) equation of state. A significant new result from our opacity calculations is a large opacity enhancement in the 20-40 eV temperature range. This new opacity bump is a result of improved atomic physics and is due to detailed term structure in iron; not included in earlier calculations. It is well known that opacity bumps can be the mechanism for pulsational instability and several groups have studied this issue using the OPAL opacities. A brief discussion of the results of these studies will be given.

RADIATIVE COLLAPSE OF A DENSE PLASMA

N. Rostoker
Department of Physics, University of California at Irvine

Radiative collapse was first proposed by Pease[1] and Braginskii for Z-pinches of Hydrogen in a Bennett type equilibrium. Ohmic heating decreases with current I like (1/I) and Bremstrahlung increases like I. If the current exceeds the value $I_c = 1.66$ M. amps the radiation dominates, the plasma should be radiation cooled causing collapse if the current and magnetic pressure are maintained. The collapse would cease when the absorption length becomes comparable with the plasma radius. The current required for radiative collapse can be much less for higher Z-plasmas such as Krypton,[2] or for hydrogen seeded with high Z-impurities.[3]

There is experimental evidence of radiative collapse for Z-pinches seeded[4] with high Z-impurities, for vacuum sparks,[5] and a plasma focus[6] seeded with high Z-impurities. In the latter case there are indications that in regions of very small size of the order of 1 micron, densities of the order of 10^{24} cm^{-3} were attained, which is comparable to that achieved by implosions with the Nova laser at LLNL.

Recently there have been Z-pinch experiments of a solid fiber, or cryogenic deuterium fiber. The initial inductance of such fibers is large and the current rise time is at least 10's of nanoseconds. The plasma expands until the magnetic pressure is sufficiently large to contain the material pressure and the plasma eventually becomes unstable without achieving very high density. A solution to these problems is proposed that involves a Z-θ pinch.[7] In this hybrid scheme an annular Z-pinch plasma implodes an axial B_z-magnetic field compressing it to multi-megagauss fields with an order of magnitude shorter rise time than the Z-current. Coaxial with the Z-pinch is a solid fiber or straw which breaks down and forms a θ-pinch. The rise time of the current in the θ–pinch is a few nanoseconds and the Z-θ configuration is much more stable than a simple Z-pinch.

REFERENCES

1. S. I. Braginskii in Plasma Physics and The Problem of Controlled Thermonuclear Fusion, Pergamon Press (1961), p. 135; R. S. Pease, Proc. Phys. Soc. London B **70**, 11 (1957).

2. J. P. Apruzese and P. C. Kepple, Proc. 2nd Int. Conf. on High Density Pinches, Laguna Beach, April 26 - 29 (1989).

3. J. W. Shearer, Phys. Fluids **19**, 1426 (1976).

4. J. Bailey, Y. Ettinger, A. Fisher and N. Rostoker, Appl. Phys. Lett. **40**, 460 (1982); J. Appl. Phys. **60**, 1939 (1986).

5. E. Ya Gol'ts et al., Phys. Lett. A **115**, 114 (1986); Phys. Lett. A **119**, 359 (1987).

6. K. N. Koshelev et al., J. Phys. D - Appl. Phys. **21**, 1827 (1988) (printed in U.K.)

7. H. U. Rahman, P. Ney, F. J. Wessel, A. Fisher and N. Rostoker, Proc. 2nd Int. Conf. on High Density Pinches, Laguna Beach, April 26 - 29 (1989), AIP Conf. Proc., p. 195.

Nuclear Energy in an Atomic Lattice: Causal Order

Julian Schwinger
Department of Physics, University of California
Los Angeles, CA 90024, U.S.A.

The extremely small penetrability of the Coulomb barrier is generally adduced to dismiss the possibility of low energy (cold) fusion. The existence of other mechanisms that could invalidate this logic is pointed out.

The idea that adjacent isotopes of hydrogen, bound within a palladium lattice, can undergo significant nuclear reactions is generally dismissed as a violation of known physical laws. That conviction is based largely on the extremely small probability, as conventionally estimated, for penetrating the Coulomb barrier with energies at the atomic level. Implicit in this line of thought is the apparently self-evident causality assignment that has the release into the surrounding environment, of energy at the nuclear level, occur after the penetration of the Coulomb barrier. One would hardly question that time sequence when the environment is the vacuum. But does it necessarily apply to the surrounding ionic lattice?

To set the stage for a response, I quote from a paper delivered at the Yoshio Nishina Centennial Symposium[1]:

". . . the loading of deuterium into the palladium lattice does not occur with perfect spatial uniformity. There are fluctuations. It may happen that a microscopically large – if macroscopically small – region attains a state of such lattice uniformity that it can function collectively in absorbing the excess nuclear energy that is released in an act of fusion."

It would seem that conventional causality is assumed here. But, another reading is possible, one in which the causal order is reversed. Why? Because, in contrast with the vacuum, the lattice is a dynamical system, capable of storing and exchanging energy.

The initial stage of the new mechanism can be described as an energy fluctuation, within the uniform lattice segment, that takes energy at the nuclear level from a pd or dd pair and transfers it to the rest of the lattice, leaving the pair in a virtual state of negative energy. This general characterization becomes more explicit in the language of phonons. The non-linearities associated with large displacements constitute a source of the phonons of the small amplitude, linear regime. Intense phonon emission can leave the particle pair in a virtual negative energy state.

For the final stage of the new mechanism, consider the pd example where there is a stable bound state: ^{3}He. If the energy of the virtual state nearly coincides with that of ^{3}He, a resonant situation exists, leading to amplification, rather than Coulomb barrier suppression.

It would seem that two mechanisms are available, characterized

by different causal orderings. But are they not extreme examples of mechanisms that in general possess no particular causal order?[1]:

". . . one is dealing, essentially, with a single wavefunction, which does not permit such factorization."

It is not my intent – nor would I be qualified – to declare the reality of the evidence offered for what has been called cold fusion. Rather, I only point out that the argument that has produced contemptuous dismissal of the possibility could be based on a false premise. The subject requires research, not fiat.

---

1) J. Schwinger, Cold Fusion – Does It Have a Future? in Evolutional Trends of Physical Science (Springer-Verlag, 1991).

A COMMUNICATION WITH PROFESSOR TAJIMA

DENSE PLASMAS PRODUCED FROM SOLID DEUTERIUM Z-PINCHES

Jack S. Shlachter

Physics Division
Los Alamos National Laboratory
Los Alamos, NM 87545

Abstract

For the past six years, our group at Los Alamos has conducted a series of magnetic fusion, pulsed-power experiments that use a cryogenic fiber of deuterium as the initial load. These experiments were motivated by an analysis of the dynamics of a simple, linear z-pinch subject to two constraints: 1) pressure balance between the self-generated azimuthal magnetic field and the plasma internal pressure, and 2) power balance between ohmic heating input and bremsstrahlung losses. This analysis indicates the desirability of operation in the high density, small radius, short time scale regime and necessitated the development of techniques to produce frozen deuterium fibers in vacuum with characteristic radii of 15 microns. These fibers span the 5 cm anode-cathode gap on a pulsed power device (HDZP-II) with the capability of delivering 1 MA of current to an inductive load with a rise time of 100 ns. The stored energy in HDZP-II is 200 kJ and the output of the Marx bank generator is pulse-compressed before reaching the load chamber.

The results from a variety of diagnostics are consistent with the conclusion that the plasma column expands during the first 10 ns of the current rise as a result of the rapid development of an m=0 instability. A single frame Mach-Zehnder interferogram provides the most direct evidence for this MHD activity and indicates the presence of plasma at radii as great as 1 mm early during the current pulse. Neutron activation detectors substantiate this view, as the measured neutron yield (10^9 - 10^{10} per pulse) is significantly below the value expected for a plasma column which remains confined at solid or near solid densities. Time-resolved neutron emission data are provided by a scintillator-photomultiplier combination which displays a broad, 50 ns pulse. An array of PIN diodes with thin metallic foil filters are used to produce a temporally resolved measurement of the x-ray spectrum. Two distinct features are observed, an early, relatively soft pulse with characteristic energies of tens of kV, and a later, hard pulse of several hundred keV x rays. A time-integrating x-ray pinhole camera has also been employed, and images of a reasonably uniform emitting column have been obtained.

STRUCTURE FORMATION IN DENSE COSMOLOGICAL PLASMAS

T. Tajima, S. Cable and S. Oliveira

Department of Physics
and
Institute for Fusion Studies
The University of Texas at Austin

ABSTRACT

It is shown that a plasma with temperature T sustains fluctuations of electromagnetic fields and particle density even if it is assumed to be in a thermal equilibrium. The level of fluctuations in the plasma for a given wavelength and frequency of electromagnetic fields is rigorously computed by the fluctuation-dissipation theorem. A large zero frequency peak of electromagnetic fluctuations is discovered. We show that the energy contained in this peak is complementary to the energy "lost" by the plasma cutoff effect. The level of the zero (or nearly zero) frequency magnetic fields is computed as $(B^2)_0/8\pi = \frac{1}{2\pi^3} T(\omega_p/c)^3$, where T and ω_p are the temperature and plasma frequency. The level of magnetic fields is significant at the early radiation epoch of the Universe, particularly for $t = 10^{-2}$–10^0 seconds after the Big Bang, during which the magnetic fluctuations are as great as or even greater than the plasma pressure. This leads to a possibility of strongly nonuniform plasmas in this epoch of the Universe. The subsequent consequence of such magnetic fields includes the "polymerization" of magnetic fields to generate larger (and in fact large) magnetic structures during the radiation epoch. A possible significant consequence of this is a creation of large cosmological structures prior to the recombination and the annihilation of the Sachs-Wolfe effect. In addition, such large fluctuations may impact nucleosynthesis.

Preliminary Results of Cold Fusion Experiment from Kamiokande

Presented by M. Takita
Osaka University
October 7, 1991

After reports[1],[2],[3] of observation of "cold fusion", tremendous efforts are being made to clarify the phenomena. Nonetheless, cold fusion has not been confirmed yet. The basic reactions of the signature is summarized as:

(1) d+d$\rightarrow^3$He(0.82 MeV)+n(2.45 MeV)

(2) d+d$\rightarrow$t(1.01 MeV)+p(3.02 MeV)

(3) p+d$\rightarrow^3$He+γ(5.49 MeV)

Most of the experiments try to detect the neutron in the reaction (1) or the tritium in the reaction (2). The Kamiokande III experiment uses the reaction (1) for detecting the signature. We decide to do the experiment (with various forms of Pd and Ti metal in D_2O electrolysis cells and in D_2 gas pressurized cells) in collaboration with the Brigham Young University group, the Los Alamos National Laboratory group, and the Texas A & M group. The existing experiments argue the continuous neutron emission rate of $10^{-2}\sim10^{-1}$ n/sec and time-correlated neutron bursts 10$\sim$a few $\times$100 n of $\leq$ 100 μsec duration (burst rate $\sim$ a few / 10^3 hours). The sensitivity to the continuous neutron emission is limited by the environmental or cosmic-ray background. In order to settle down the situation, it is necessary to carry out experiments with much less background.

Kamiokande III, an upgraded version of Kamiokande II[4], is an imaging water Čerenkov detector located 1000 m underground (2700 meters of water equivalent) in the Kamioka metal mine in the Gifu prefecture of Japan, at 36.4°N, 137.3° and 25.8°N geomagnetic latitude. The main improvement is the replacement of dead PMTs, the installation of new electronics system and of small mirrors surrounding each PMT to increase the light collection efficiency ($\sim$30 % increase). The detector consists of an inner main detector (3000 tons) and an outer anticounter (1500 tons). The inner detector is contained in a cylindrical steel tank and has a cylindrical photosensitive volume, 14.4 m in diameter $\times$ 13.1 m in height, containing 2142 tons of water. A total of 947 photomultipliers (PMTs).

each with 50 cm ϕ photosensitive area, cover 20 % of the entire inner surface of the water tank. The fiducial mass for the continuous neutron emission (the burst emission) is a sphere with a radius of 2m (3.5m) at the detector center. A 10-MeV electron gives an average ~40 PMT hits. The trigger threshold is now estimated to be ~5 MeV at 50 % efficiency. At the center of the detector, where the fusion cells are to be placed, environmental neutrons are almost completely absorbed by the 4500 tons of water.

The neutron is detected in the Kamiokande III detector through the $^{35}Cl(n,\gamma)^{36}Cl$ reaction. The cold fusion cells are placed in a acrylic vessel containing ~20 % NaCl water solution. The vessel is then located at the center of the Kamiokande III detector. Neurons are thermalized in the solution and absorbed in ^{35}Cl and converts themselves into γ's with their energies up to 8.6 MeV (~70 % above 6 MeV). Therefore, the cold fusion signal appears as 6~8.6 MeV γ rays with their vertex position being located near the center of the detector. The vertex position resolution is 1~1.5 m for the γ rays. A test experiment was done in January 1991. The neutron detection efficiency is estimated to be ~20 % by means of calibrated neutron fission sources. The background rate above 6 MeV is ~1 event/4 hour. The sensitivity to the cold fusion neutrons is as low as $\sim 10^{-4}$ n/sec, assuming a S/N ratio of 1. Since April 1991, the cold fusion experiment has been running. At this workshop, some preliminary results of the experiment will be reported.

References

[1] S. E. Jones et al., Nature 338 (1989) 737.

[2] A. Bertin et al., Nuovo Cimento 101A (1989) 997.

[3] H. O. Menlove et al., Journal of Fusion Energy 9 (1990) 495.

[4] See, for example, K.S.Hirata et al., Phys. Rev. D38 (1988) 448.

Recent Results of ^{8}B Solar Neutrino Observation from Kamiokande

Presented by M. Takita
Osaka University
October 9, 1991

1. Introduction

The Kamiokande II experiment is dedicated to the detection for nucleon decays as well as to the neutrino astronomy. In this report, we will present recent results of ^{8}B solar neutrino (end point energy = 14 MeV) observation from the Kamiokande II experiment, based on 1040-day (January 1987 – April 1990) data. ^{8}B solar neutrinos are measured in the Kamiokande II by detecting a recoil electron off $\nu_e e \rightarrow \nu_e e$ elastic scatterings. Kamiokande II provides, therefore, a real time measurement of directional information of the recoil electrons with respect to the Sun as well as of energy spectrum of them.

A primary motivation of the study of solar neutrinos is the prospect that it will directly reveal the inner structure of the Sun. At the same time, it may also reveal as yet undetected intrinsic properties of neutrinos, owing to the wide range of matter density, the very long distance from the Sun to the Earth, and the relatively high magnetic field traversed by low-energy solar neutrinos in their passage from the center of the Sun to a detector on earth.

2. Kamiokande II detector

Kamiokande II is an imaging water Čerenkov detector located 1000 m underground (2700 meters of water equivalent) in the Kamioka metal mine in the Gifu prefecture of Japan, at 36.4°N, 137.3° and 25.8°N geomagnetic latitude. The detector consists of an inner main detector (3000 tons) and an outer anticounter (1500 tons). The inner detector is contained in a cylindrical steel tank and has a cylindrical photosensitive volume, 14.4 m in diameter × 13.1 m in height, containing 2142 tons of water. A total of 948 photomultipliers (PMTs), each with 50 cm ϕ photosensitive area, cover 20 % of the entire

inner surface of the water tank. The fiducial mass for the ^{8}B solar neutrino measurement is 680 tons. The 1040-day data sample is divided into 2 subsamples; 450-day (590-day) subsample before (after) PMT gain doubling at an analysis threshold of 9.3 (7.5) MeV. A 10-MeV electron gives an average 26 (30) PMT hits before (after) PMT gain doubling.

3. Physics results

(i) Measurement of ^{8}B solar neutrino flux and search for short-term time variation of the flux[1],[2]

A data sample of 1040 days from the Kamiokande II detector, consisting of subsamples of 450 days at electron-energy threshold $E_e \geq 9.3$ MeV and 590 days at $E_e \geq 7.5$ MeV, yields a clear directional correlation of the solar-neutrino-induced electron events with respect to the Sun and a measurement of the differential electron-energy distribution. These provide unequivocal evidence for the production of ^{8}B by fusion in the Sun. The measured flux of ^{8}B solar neutrinos from the two subsamples relative to a prediction of the standard solar model is $0.46 \pm 0.05(\text{stat}) \pm 0.06(\text{syst})$. The total data sample is tested for short-term time variation; within the statistical error, no significant variation is observed.

(ii) Constraints on neutrino-oscillation parameters[1],[3]

An analysis of the Mikheyev-Smirnov-Wolfenstein effect using 1040 days of Kamiokande-II data is reported, which provides constraints on neutrino-oscillation parameters. The measured recoil-electron energy spectrum alone leads to the conclusion that the adiabatic region, $7.2 \times 10^{-4} < \sin^2 2\theta < 6.3 \times 10^{-3}$, $\Delta m^2 \sim 1.3 \times 10^{-4}$ (eV^2), is disfavored at the 90 % confidence level.

(iii) Search for day-night and semiannual variations in the solar neutrino flux[1],[4]

Search for possible day-night and semiannual variations of the ^{8}B solar neutrino flux are reported based on 1040 days of Kamiokande-II data. Within statistical error, no such

short-time variations were observed. The limit on the day-night difference sets a constraint on neutrino-oscillation parameters. A region defined by $\sin^2 2\theta \geq 0.02$ and $2 \times 10^{-6} \leq \Delta m^2 \leq 10^{-5}$ eV^2 is excluded at 90 % C.L. without any assumption on the absolute value of the expected solar neutrino flux.

References

[1] K.S.Hirata et al., ICRR-Report-245-91-14, July 1991, submitted to Physical Review D.

[2] K.S.Hirata et al., Phys. Rev. Lett. 65 (1990) 1297.

[3] K.S.Hirata et al., Phys. Rev. Lett. 65 (1990) 1301.

[4] K.S.Hirata et al., Phys. Rev. Lett. 66 (1991) 9.

He-"Burning" at $T = 0$ and Ultra-High Densities

H. M. Van Horn[1], S. Ogata[1,2], and S. Ichimaru[1,2]

Abstract

He burning at finite temperature is well-known to proceed through three stages (*cf.* Clayton 1968 and references therein): $^4\mathrm{He} + {}^4\mathrm{He} + 92\mathrm{keV} \rightleftharpoons {}^8\mathrm{Be}$; $^4\mathrm{He} + {}^8\mathrm{Be} + 278\mathrm{keV} \rightleftharpoons {}^{12}\mathrm{C}^*$; and $^{12}\mathrm{C}^* \rightarrow {}^{12}\mathrm{C} + 7.644\mathrm{MeV}$. The energy differences in these reactions are conventionally calculated solely as mass differences between the reactants and the product nuclei. However, at high densities, the mass difference is only one part of the relevant energy difference; the most important additional term is the difference in the Coulomb energies of the nuclei and their neutralizing electrons (*cf.* Salpeter 1961, Baym *et al.* 1971, Shapiro & Teukolsky 1983, p. 49 ff.). At sufficiently high matter densities, such as may occur in the dense surface layers of slowly accreting neutron stars, the larger (negative) Coulomb interaction energy of the ^{8}Be nucleus and its screening electrons is enough greater than the energy of two ^{4}He nuclei and their electrons so that the ground state of ^{8}Be becomes stable against decay into two α-particles. This occurs at a mass density $\rho \approx 5.5 \times 10^9$ g cm^{-3}. Above this density, pure He matter in its ground state would undergo a spontaneous "phase transition" to a stable, ^{8}Be ground state. The character of He burning is thus very different at high densities and low temperatures than is indicated by calculations of the 3α rate enhanced by screening and many-body effects (*cf.* Ogata *et al.* 1991), which are appropriate at finite temperatures.

In this paper we discuss two possibilities for the He-"burning" reactions at $T = 0$. (1) If electron captures at these high densities can be neglected, He-"burning" at $T = 0$ may proceed *via* successive "phase transitions," beginning with $^4\mathrm{He} + {}^4\mathrm{He} \rightarrow {}^8\mathrm{Be}$ ($\rho \geq 5.5 \times 10^9$ g cm^{-3}). (2) Because these densities are so high, however, it seems more likely that He-"burning" at $T = 0$ may proceed instead through a series of electron capture reactions, and we present a series of such reactions. Calculations of the reaction rates for these processes are currently in progress.

Acknowledgements

We thank D. S. Koltun for several helpful discussions. This work has been supported in part by the National Science Foundation under grant INT 90-16293 through the University of Rochester and in part by the Japanese Ministry of Education and by the Japan Society for the Promotion of Science through the respective Research Grants to the University of Tokyo.

References

Baym, G., Pethick, C., and Sutherland, P. 1971, *Ap. J.*, **170**, 299.

Clayton, D. D. 1968, *Principles of Stellar Evolution and Nucleosynthesis*, (McGraw-Hill: New York).

Ogata, S., Ichimaru, S., and Van Horn, H. M. 1991, these proceedings.

Salpeter, E. E. 1961, *Ap. J.*, **134**, 669.

Shapiro, S. L., Teukolsky, S. A. 1983, *Black Holes, White Dwarfs, and Neutron Stars* (Wiley: New York)

[1] Department of Physics and Astronomy and C. E. Kenneth Mees Observatory, University of Rochester, Rochester, NY 14627-0011

[2] Department of Physics, University of Tokyo, Bunkyo-ku, Tokyo 113, Japan

MODEL FOR CLUSTER IMPACT FUSION*

James P. Vary, Charles J. Benesh and John R. Spence
Department of Physics and Astronomy
Iowa State University
Ames, IA 50011

We present a model in which the anomalously large cluster impact fusion yields, initially reported by Beuhler, Friedlander and Friedman (Phys. Rev. Lett. **63**, 1292(1989)), may be understood in terms of the formation of one or more previously unobserved resonances in the electron-deuteron system with energies in the range 0 - 1 eV. The theory of resonances in the electron-proton system (J.R. Spence and J.P. Vary, Physics Letters B, to appear) will be outlined as motivating the model. These e-p resonant states are compact and have very long lifetimes. Since these characteristics are distinct from typical atomic properties we refer to these resonances as states of "protonium". The compact size indicates effective screening of the coulomb repulsion leading to enhanced fusion rates. Using a simple thermodynamic model of the conditions created by the cluster impacts, we calculate the formation rate of the lowest energy electron-deuteron resonance and find that the dependence of the fusion yield on cluster energy is reasonably well reproduced for a resonance energy of 0.67 eV, and a resonance width greater than or equal to 10^{-13} eV. Suggestions for further tests of the model will be presented.

*Supported in part by the US Department of Energy under contract No. DE-FG02-87ER40371, Division of High Energy and Nuclear Physics, and by contract No. W7405-ENG-82

ON THE RATE OF IONIZATION IN DENSE PLASMAS

Jon C. Weisheit

Space Physics & Astronomy Department
Rice University
Houston, TX 77251 USA

Advances continue to be made in the development of high-power lasers and in the efficiency with which laser power is coupled to implosion targets: plasma densities N_e in excess of 10^{25} electrons/cm^3 have now been achieved. Atomic ions are strongly perturbed by such an environment, in which the mean inter-electron separation is less than a Bohr radius. Because spectroscopy provides the most detailed information on these non-LTE implosion plasmas, the understanding of how a dense plasma modifies atomic collisional and radiative processes remains an important subject of research.

During the past several years, and with various collaborators, this author has carried out a series of studies of dense plasma effects on atomic collisions; these focussed on bound-state excitations by ion and by electron impact. The focus of the present research is on electron-impact excitations to the continuum, *i.e.*, ionizations. As in the case of bound-bound transitions, one key issue is how to handle the simultaneous interactions of a target ion with a large number of plasma electrons. We have decided first to extend the formalism we developed for excitation via plasma fluctuations to treat ionizations too. In this fluctuation model, the traditional concept of a cross section (which eventually is averaged with respect to a distribution of incident electron speeds to produce a rate coefficient, and then multiplied by N_e to obtain a transition probability per unit time) is dropped in favor of a direct calculation of the probability of a transition due to stochastic changes in the plasma's local electric field. These changes are fully characterized by the plasma's dynamic structure factor $S_{ee}(k,\omega)$.

The general, first-order expression we have derived for the probability of ionizing a hydrogenic ion in state "n" is an iterated integral involving the product of $S_{ee}(k,\omega)$ and the generalized oscillator strength per unit (continuum) energy interval, df_n/dE. At present, we are carrying out numerical calculations for a variety of approximations to the plasma structure factor -- weak or strong Coulomb coupling, dynamic or static response, plus different approximations to the oscillator strength density, including a binary encounter formula and Fock's plane-wave formula.

Our main goal is to establish the extent to which high plasma density modifies the rate of ionization of excited ionic levels, especially those near the continuum, as well as to determine the accuracy of the several simplifications listed above. We hope also to make a formal connection between this work and recent studies of the enhancement of three-body recombination rates by collective effects (plasmon emission) in dense, cool plasmas. And, finally, we intend to investigate the importance of different choices for the "continuum lowering" by the surrounding plasma. The oral presentation will summarize our progress along these lines.

Thermonuclear Carbon Ignition in Electron Degenerate Stars

J. Craig Wheeler
Department of Astronomy
University of Texas at Austin

and

Zalman Barkat
Department of Physics
Hebrew University of Jerusalem

Type Ia supernova and related events are widely regarded to be the result of the thermonuclear ignition of carbon under conditions of extremely high density and electron degeneracy. The condition for carbon ignition is that the energy generation rate from strongly screened carbon burning reactions should exceed the neutrino loss and hence cooling rate that derives from a number of physical mechanisms, especially plasmon excitations and neutrino bremsstrahlung. Standard calculations of the relevant physical rates suggest that carbon ignition occurs at about 3×10^9 gm cm^{-3}. At this density, however, convection breaks out and a new neutrino cooling process, the convective Urca process, becomes an efficient coolant. The result is that the thermonuclear runaway is postponed to significantly higher density and the higher density leads to significantly higher weak interaction rates in the burned material. The subsequent neutronization leads to the ejection of an excess of highly neutron rich species. This result could be avoided if the threshold for carbon ignition were slightly smaller, less than $\sim 1.4 \times 10^9$ gm cm^{-3}, the threshold for the Urca process on the dominant seed nucleus, ^{23}Na. It is of great interest to examine the uncertainties in the current calculations of electron screening, which enhances the nuclear reaction rates, and the neutrino cooling processes to see if an ignition density of $< 1.4 \times 10^9$ gm cm^{-3} is feasible. If so, carbon ignition would lead to a brief convective phase before full dynamical runaway, but the convective Urca process would be avoided and runaway would occur at essentially the ignition density, thus avoiding excess neutronization. Ignition under these slightly lower density conditions would be more conducive to the generation of a supersonic detonation.

A Search For Nuclear Effects from Deuterated Metals*

K.L. Wolf, Cyclotron Institute, Texas A&M University
College Station, TX 77843

Results are presented from a research program in which several detection methods have been used to search for products and emissions from possible nuclear reactions in deuterated titanium, palladium and several alloys. Four NE213 neutron counters operating in a 8-fold multi-hit mode are used with an active cosmic ray shield for low background fast neutron detection and neutron energy spectra. Direct charged particle emission is studied with a bank of 600mm^2 silicon detectors and two sets of delta E-E silicon telescopes for particle identification. Tritium beta decay and other long-lived activities are measured with in situ liquid scintillation counting. A high resolution Ge detector and a set of large volume NaI crystals are used for gamma ray emission. A Si(Li) X-ray spectrometer is used for materials characterization with fluorescence methods. Measurements of X-ray emission and other low energy photons are made on thin Pd metal samples. Deuterium and hydrogen content is studied with elastic neutron scattering.

*This work supported by the Electric Power Research Institute, Exploratory Research Division.

Many-Atom Effects on Transport Processes in Dense Plasmas

Stephen M. Younger
Los Alamos National Laboratory
Los Alamos, NM 87545

We have studied the dynamic behavior of many-atom samples of dense matter using self-consistent field molecular dynamics (SCFMD), a synthesis of techniques from quantum chemistry and molecular dynamics. In simulations containing up to 30 atoms the electrons are described in a Hartree-Fock approximation. This charge distribution is used to compute the forces on the nuclei, which are then moved classically. By repeating these procedures over several hundred to several thousand timesteps it is possible to describe the time evolution of the sample. Approximate periodic boundary conditions include the effect of extended media.

At densities where the interatomic spacing is comparable to the atomic radius quasi-molecular structures form and the interatomic force differs considerably from the superposition of isolated pair potentials. This orbital hybridization can affect the ionic transport as well as the electronic properties of the material. Note that these effects are due to changes in the interatomic force, not simply many-atom interactions.

Calculations of the self-diffisuion rate have been performed on helium over the density range 0.1-8.0 g/cc to illustrate the departure of the kinetics from pair approximation models. In a study of dense hydrogen we found that above 0.25 g/cc distinct planar structures formed in the simulations, suggestive of the formation of an ordered solid phase which persists until remarkably high temperatures.

Current work includes the application of various time dependent quantum approximations to study reactive processes in solid matter and screening effects in hot dense plasma.

V. ADDRESS LIST

1991 US–JAPAN WORKSHOP ON NUCLEAR FUSION IN DENSE PLASMAS

October 7-9
Joe C. Thompson Conference Center
The University of Texas at Austin

ORGANIZERS

T. TAJIMA
Institute for Fusion Studies
The University of Texas at Austin

S. ICHIMARU
Department of Physics
University of Tokyo

SPEAKERS AND TOPICS

John F. Benage, Jr.
P-1, Mail Stop E526
Los Alamos National Laboratory
Post Office Box 1663
Los Alamos, New Mexico 87545
505-667-8900

Electrical Resistivity of a Dense Polyurethane Plasma

F. Edward Cecil
Department of Physics
Colorado School of Mines
Golden, Colorado 80401
303-273-3736

Gamma-rays and Charged Particle Studies from Dense Plasmas

Michael C. Downer
Department of Physics
The University of Texas at Austin
Austin, Texas 78712
512-471-6054

Dense Plasmas Created by Femtosecond Laser Pulses

Peter L. Hagelstein
Dept. of Electrical Engineering & Computer Science
Building 38, Room 290
Massachusetts Institute of Technology
77 Massachusetts Avenue
Cambridge, Massachusetts 02139
617-253-0899

Coherent and Semi-Coherent Neutron Transfer Reactions

Richard D. Hazeltine
Institute for Fusion Studies
The University of Texas at Austin
Austin, Texas 78712
512-471-1322

Opening Remarks

Setsuo Ichimaru
Department of Physics
University of Tokyo
7-3-1 Hongo, Bunkyo-ku, Tokyo 113, Japan
f: 03-3814-9717; t: 03-3812-2111 x 4248

Nuclear Fusion in Dense Plasmas–Supernovae to Ultrahigh-Pressure Liquid Metals
Liquid Metallic Hydrogen–Equation of State, Transport, and Impurity Ionization

Naoki Itoh
Department of Physics
Sophia University
7-1 Kioicho, Chiyoda-ku, Tokyo 102, Japan
f: 03-3238-3341; t: 03-3238-3431

Neutrino Energy Loss in Dense High-Temperature Stars

Hiroshi Iyetomi
Department of Physics
University of Tokyo
7-3-1 Hongo, Bunkyo-ku, Tokyo 113, Japan
f: 03-3814-9717; t: 03-3812-2111 x 4249

Freezing Transitions and Phase Separations in Dense Multi-Ionic Plasmas

Steven E. Jones
Department of Physics & Astronomy
Brigham Young University
296 Eyring Science Center
Provo, Utah 84602
801-378-2749 (fax: 801-378-2265)

Anomalous Nuclear Effects in Deuterided Solids–Preliminary New Results

Irvin R. Lindemuth
X-1, MS F645
Inertial Fusion and Plasma Theory
Los Alamos National Laboratory
Los Alamos, New Mexico 87545

High Density Cryogenic Fiber Z-Pinch

Swadesh Mahajan
Institute for Fusion Studies
The University of Texas at Austin
Austin, Texas 78712
512-471-4376

Modes in Gluon and Quark-Gluon Plasmas

Richard A. Matzner
Department of Physics
The University of Texas at Austin
Austin, Texas 78712
512-471-5062

Baryon Inhomogeneities and the Primordial Light-Element Abundances

Michael McKubre
Chemical Physics Lab
Stanford Research Inst. Intnl.
333 Ravenswood Avenue
Menlo Park, California 94025
415-859-3868

Electrochemistry and Calorimetry of the D/Pd System

George H. Miley
214 Nuclear Engineering Laboratory
University of Illinois at Urbana-Champaign
103 South Goodwin Avenue
Urbana, Illinois 61801
217-244-4947

Dense Core Plasma in an Inertial Electrostatic Confinement Device

Richard M. More
L-321, T Group
Physics Department
Lawrence Livermore National Laboratory
Post Office Box 5508
Livermore, California 94550
415-422-7208

Semiclassical Calculation of Dense Plasma Physics

Katsunobu Nishihara
Institute of Laser Engineering
Osaka University
2-6 Yamadaoka, Suita, Osaka 565, Japan
f: 06-877-4799; t: 06-877-5111 x 6545

Nonlinear AC Conductivity of Solid Density Plasma
Effect of Radiative Processes on Radiation Transport

Shuji Ogata
Department of Physics
University of Tokyo
7-3-1 Hongo, Bunkyo-ku, Tokyo 113, Japan
f: 03-3814-9717; t: 03-3812-2111 x 4125

Nuclear Reaction Rates in Dense Multi-Ionic Stellar Materials

Forrest J. Rogers
V Division, L-296
Lawrence Livermore National Laboratory
Post Office Box 808
Livermore, California 94550
415-422-7351

Opacity in Stellar Plasmas

Norman Rostoker
Department of Physics
University of California Irvine
Irvine, California 92717
714-856-6949

Radiative Collapse of a Dense Plasma

Jack S. Shlachter
P-1, Mail Stop E526
Los Alamos National Laboratory
Post Office Box 1663
Los Alamos, New Mexico 87545
505-665-2985

Dense Plasmas Produced from Solid Deuterium Z-Pinches

Toshiki Tajima
Institute for Fusion Studies
The University of Texas at Austin
Austin, Texas 78712
512-471-4574

Masato Takita
Physics Deparment
Osaka University
1-1 Machikaneyama, Toyonaka, Osaka 560, Japan
f: 06-855-6664; t: 06-844-1151 x 4132-3

Recent Results of ^8B Solar Neutrino Observation from Kamiokande
Preliminary Results of Cold Fusion Experiment from Kamiokande

Hugh M. Van Horn
Department of Physics and Astronomy
University of Rochester
Rochester, New York 14627
716-275-5928

He- "Burning" at T = 0 and Ultra-High Densities

James P. Vary
Department of Physics
Iowa State University
Ames, Iowa 50011
515-294-3877

Model for Cluster Impact Fusion

Jon Weisheit
Department of Space Physics and Astronomy
Rice University
Post Office Box 1892
Houston, Texas 77251
713-527-8101 x 3425

On the Rate of Ionization in Dense Plasmas

J. Craig Wheeler
Department of Astronomy
The University of Texas at Austin
Austin, Texas 78712
512-471-6407

Thermonuclear Carbon Ignition in Electron Degenerate Stars

Kevin L. Wolf
Cyclotron Institute
Texas A & M University
College Station, Texas 77843-3366
409-845-1411

Stephen M. Younger
Inertial Fusion and Plasma Theory
X-1, Mail Stop F-645
Los Alamos National Laboratory
Post Office Box 1663
Los Alamos, New Mexico 87545
505-667-7793

Many-Atom Effects on Transport Processes in Dense Plasmas

PARTICIPANTS

Allen J. Bard
Department of Chemistry
The University of Texas at Austin
Austin, Texas 78712

David Barnett
Institute for Fusion Studies
The University of Texas at Austin
Austin, Texas 78712

Alexei Beklemishev
Kurchatov Inst. of Atomic Energy
46 Ulitsa Kurchatov
Post Office Box 3402
Moscow 123 182, USSR

Herbert L. Berk
Institute for Fusion Studies
The University of Texas at Austin
Austin, Texas 78712
512-471-1364

Samuel C. Cable
Institute for Fusion Studies
The University of Texas at Austin
Austin, Texas 78712

Isaac Chuang
Research Lab Elec 38-298
MIT
77 Massachusetts Avenue
Cambridge, Massachusetts 02139

John Cobb
Institute for Fusion Studies
The University of Texas at Austin
Austin, Texas 78712

Wendell Horton
Institute for Fusion Studies
The University of Texas at Austin
Austin, Texas 78712
512-471-1594

W. Jevtic
Cyclotron Institute
Texas A & M University
1 Spence Street
College Station, Texas 77843-3366

Samuel Oliveira
Institute for Fusion Studies
The University of Texas at Austin
Austin, Texas 78712

Takeshi Udagawa
Department of Physics
The University of Texas at Austin
Austin, Texas 78712

Peter Yushmanov
Kurchatov Inst. of Atomic Energy
46 Ulitsa Kurchatov
Post Office Box 3402
Moscow 123 182, USSR

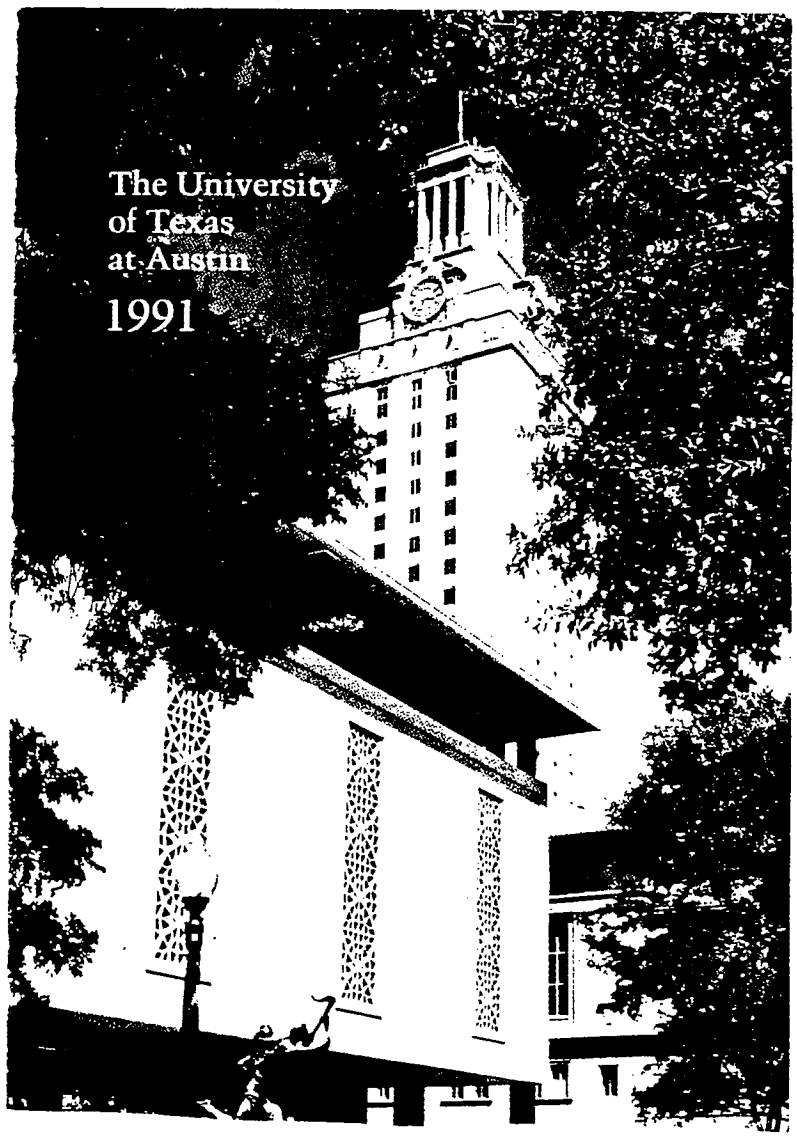
The University
of Texas
at Austin
1991